*nanomanufacturing*

*Review*

# Industrial Manufacturing Applications of Zinc Oxide Nanomaterials: A Comprehensive Study

**Md Abdus Subhan *, Newton Neogi and Kristi Priya Choudhury**

Department of Chemistry, Shahjalal University of Science and Technology, Sylhet 3114, Bangladesh
* Correspondence: subhan-che@sust.edu

**Abstract:** Nanomaterials (NMs) that are created with zinc oxide are very valuable for a wide variety of applications. There is a present interest in ZnO nanoparticles in a wide range of industries. This interest may be attributed to the fact that ZnO NPs have many important features. It will be necessary for ZnO NPs to possess certain qualities in order for them to rapidly find uses in industry and for these applications to have an effect on the expansion of the economy. A large surface area, a large bandgap, photocatalytic property, biosensing, bioimaging, and other qualities are included in this list. In this article, the extraordinary characteristics of ZnO NPs, as well as their novel applications in industrial settings and the challenges that come along with their utilization, will be discussed.

**Keywords:** nanomaterials; ZnO NPs; industrial applications; nanostructures; large bandgap

check for updates

**Citation:** Subhan, M.A.; Neogi, N.; Choudhury, K.P. Industrial Manufacturing Applications of Zinc Oxide Nanomaterials: A Comprehensive Study. *Nanomanufacturing* **2022**, *2*, 265–291. https://doi.org/10.3390/nanomanufacturing2040016

Academic Editor: Andres Castellanos-Gomez

Received: 19 October 2022
Accepted: 28 November 2022
Published: 5 December 2022



## 1. Introduction

Nanomaterials have been employed in a wide range of applications, including medical, food processing, fuel engineering, cosmetic products, textile industries, agricultural, electrical devices, automobile manufacturing, and aerospace engineering [1–4]. NPs are utilized both in academics and in industry for their suitable characteristics, unique design capabilities, ecofriendliness, ease of manufacturing, and low price [5]. NPs incorporated into a matrix of specific materials (polymer, metal, or ceramics) introduce additional novel characteristics, such as excellent mechanical stability (in terms of stability, toughness, strength, dimension, flexibility, and so on), good flame retardancy, optical features, high electro-thermal conductivity, and low water/gas permeability [6]. Due to their potential to be employed in a number of downstream applications, ZnO nanoparticles are one of the most investigated materials [7]. After iron, ZnO NPs are the second most common metal oxide, and they are cheap, safe, and simple to produce [8]. Modifying the shape of ZnO NPs and utilizing various synthesis methods, precursors, or materials to create NPs may readily change their physical and chemical characteristics [9]. ZnO NPs are used in analytical sensing because they are inorganic Group II–IV semiconductors [10]. ZnO NPs seem to be white particles that are not water soluble. Their outstanding chemical, electrical, and thermal stabilities are provided by the ZnO nanoparticle's 3.37 eV energy band and 60 meV bonding energy [11]. The optical and photocatalytic characteristics of ZnO NPs are also promising [12]. ZnO NPs are used in solar cells [13,14], photocatalysis [15,16], and chemical sensors [17]. ZnO NPs are also renowned for their low toxicity and strong UV-absorption, making them an excellent option for biological applications [18]. The strong and stiff structure of ZnO NPs makes them useful in the ceramic industry. When used as a surface material, ZnO NPs have many beneficial applications in the biomedical sector. Microbes naturally have a high resistance to ZnO NPs [19]. ZnO NPs are widely utilized in biological sensing, biological labeling, gene delivery, drug delivery, and also in nanomedicine [9]. ZnO has been certified by the Food and Drug Administration as a safe compound. ZnO may also solubilize in acidic medium, which opens up the possibility of using the material as multipurpose nanocarriers to help in medication delivery and releasing [20].

Biosynthesis of ZnO NPs reduces the production cost, whereas the conventional methods are expensive and use hazardous precursors [21]. Nonbiosynthetic methods can also be cheap and facile, such as synthesis through solid-state reactions [22]. The biosynthesis of ZnO NPs using leaf extraction from *P. pinnata* and rambutan peel extract is inexpensive [23,24]. It can also be produced economically from the fungus *A. potronii* [25]. Rice is one of the most widely consumed products worldwide [26], and its unconsumed biproduct is rice bran. Therefore, production of ZnO NPs using rice bran extract can be cost effective and easier [27]. The NPs of ZnO were predominantly rectangular, and their average size was approximately 50 nm. This environmentally friendly approach to synthesis is more promising than traditional chemical synthesis methods. A straightforward solvothermal technique was used to cultivate nanostructures of ZnO with several distinct morphologies, including nanopyramids, nanosheets, and NPs. Solution pretreatment has an effect on the shape of ZnO nanostructures as well as their optical characteristics [26]. Nanoscale ZnO may take on a number of different shapes and forms in natural settings. Needles, helices, nanorods, belts, wires, ribbons, and combs are all examples of one-dimensional structures. ZnO may exist in the form of two-dimensional structures, such as nanosheets/nanoplates, and nanopellets. Further, ZnO may be used in the production of a wide variety of three-dimensional formations, such as flowers, snowflakes, dandelion seeds, and other shapes [7]. The unusual blend of physiochemical properties that ZnO has is partly responsible for its increasing popularity. These characteristics include resistance to chemical and mechanical deterioration, broad radiation absorption, great catalytic activity, a high electrochemical coupling coefficient, and a nontoxic composition. Other characteristics include wide radiation absorption and a high electrochemical coupling coefficient. There is some degree of correlation between ZnO structure and its activity and properties. For example, the ZnO quantum dot's photocatalytic activity is quite high when compared to that of the other morphologies. Due to their high surface area, rapid adsorption rate, substantial charge separation, and low rates of electron and hole recombination, dots are the preferred form of photocatalysis. The photocatalytic potential, quantum confinement of photoinduced carriers, and specific (active) surface area are all impacted by the shape of the material [27]. Photocatalysis results indicated that disk-shaped hexagonal ZnO NPs displayed more photocatalytic activity than rod-shaped ZnO NPs. There has been an interest in semiconductor-based photocatalysts because of the hope that they offer for resolving environmental problems. ZnO's exceptional electrical and optical properties have garnered it a lot of attention, making it important because of its bandgap semiconductor properties [24]. The most frequent types of gram-positive bacteria are *Staphylococcus aureus* and *Escherichia coli*, and it was shown that ZnO NPs with a flower-like shape were more likely to be helpful in moderating the impacts of these bacteria. ZnO nanoflowers were discovered to have more sites capable of absorbing gas molecules than ZnO nanoplates, making them more suitable for use in gas sensing applications [22]. This article discusses many striking and state-of-the-art applications of ZnO NPs in a diversity of industrial settings.

## 2. Multi-Disciplinary Industrial Applications of ZnO NMs

Due to their unique properties, nanoparticles may be used for a variety of purposes. ZnO nanoparticles are the most widely utilized kinds of metal NPs, and their uses span a wide variety of fields, including medicine, food, agriculture, gas sensors, cosmetics, and electronics.

## 3. Antibacterial and Anti-Fungal Applications of ZnO NPs

Industries use antimicrobial and antifungal agents to prevent contamination and preserve their products by inhibiting micro-organisms [28]. It is, thus, crucial to develop more effective antimicrobial and antifungal agents for their auspicious applications in the industrial sectors. ZnO NPs exhibit promising antibacterial and antifungal properties (Figure 1). It shows excellent effectiveness against both gram-negative and gram-positive bacteria (Table 1). ZnO NPs have been demonstrated to be efficient against a broad spectrum of micro-organisms. The biocidal activity of *Bacillus subtilis* and *Escherichia coli* rose from silicon dioxide to titanium dioxide to ZnO [29]. ZnO is more bactericidal against *B. subtilis* than *E. coli* [29,30]. The MIC (minimum inhibitory concentration) ranged from 2000 to 12,500 ppm for *B. subtilis* and from 50,000 to 100,000 ppm for *E. coli*. The antimicrobial activity of Ta-doped ZnO NPs against *Staphylococcus aureus*, *Pseudomonas aeruginosa*, *E. coli*, and *B. subtilis* has been studied, and the findings indicate that adding $Ta^{5+}$ ions to ZnO improves the bacteriostasis impact of ZnO on bacteria in the dark [29]. ZnO nanoparticle powders and suspensions demonstrated antibacterial efficacy against *E. coli* and *S. aureus*. It is highly active against *S. aureus* [31]. ZnO NPs showed prevention against *P. aeruginosa*, *E. coli*, *S. aureus*, *B. cereus*, *Salmonella typhimurium*, *P. aeruginosa*, *Enterococcus faecalis*, *B. subtilis*, *Staphylococcus epidermidis*, *P. aeruginosa*, *Klebsiella pneumoniae*, *Candida albicans*, and many other bacteria [32]. The concentration of ZnO NPs has an effect on the antibacterial activity [33]. Another study showed that ZnO NPs have unique characteristics and a long life compared to organic disinfectants, which prompted their usage as an antibacterial agent. As a consequence of their high surface area-to-volume ratio, they may be used as new antibacterial agents. ZnO NPs have a high toxicity to organisms, making them a good option for antimicrobial chemistry and antimicrobio-anatomy [34].

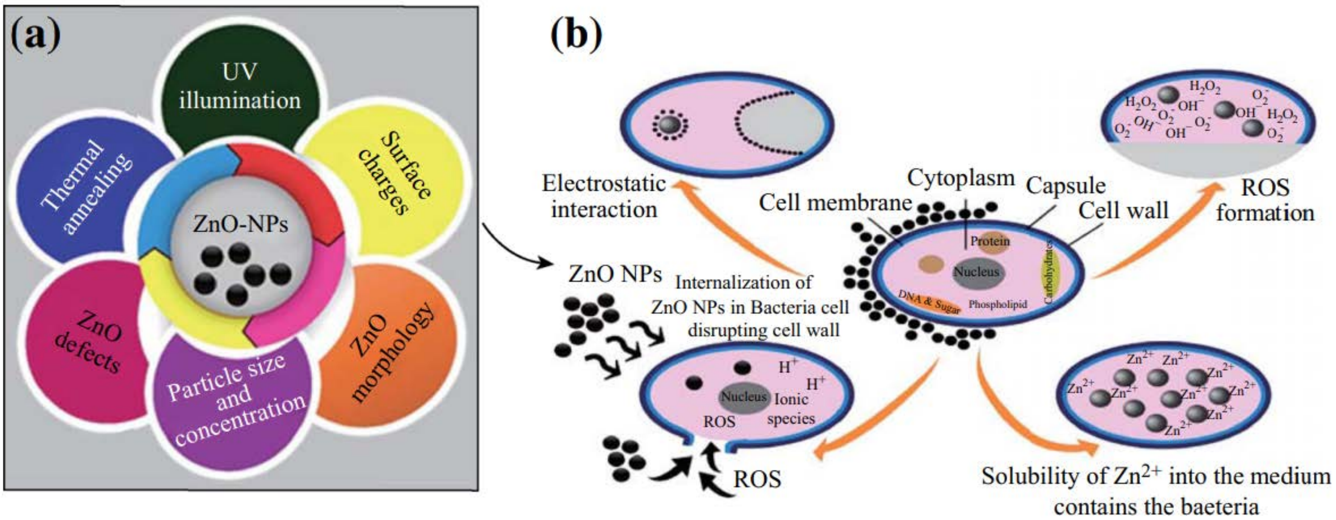


**Figure 1.** (**a**) An impact of key ZnO NPs parameters on the antibacterial response and (**b**) correlation between the several potential mechanisms of ZnO NPs antibacterial activity, such as ROS production, $Zn^{2+}$ release, internalization of ZnO NPs into bacteria, and electrostatic interactions [34].

The antibacterial activity of ZnO NPs may be related to their small size, which makes them easily adhere to the cell wall and break down the bacterial membrane, killing the cell. It has also been suggested that NPs exert their effects by releasing various levels of $H_2O_2$ and reactive oxygen species (ROS) (Figure 1). Results showed that ZnO NPs were more toxic to gram-positive bacteria than to gram-negative bacteria. This could be because gram-positive bacteria have a lower antioxidant cellular capacity, rendering them more susceptible to ROS. However, it has been suggested that the $Zn^{2+}$ ions released from the dissolution of ZnO NPs can cling to the bacterial membrane and prolong the growth phase of the bacteria [34].

Antibacterial activity of ZnO quantum dots (practically spherical and 3–7 nm) against *E. coli* was shown to be dependent on the surface-adsorbed anionic species. The antimicrobial potential of the acetate-adsorbed ZnO QDs was greater than that of the nitrate-adsorbed ZnO quantum dots under light. ZnO QDs that were nitrate-adsorbed were less effective in killing bacteria than those that were acetate-adsorbed. ZnO QDs may be able to trap electrons through the adsorption of anions on their surface. The semiconductor nature of ZnO QDs causes electron-hole pairs to form when they are exposed to light. They produce superoxide, $H_2O_2$, and hydroxyl radicals (by reactions I and II) that hinder the growth of bacteria.

$$O_2 + e^- \rightarrow O_2^-;\ H^+ + O_2^- \rightarrow \bullet HO_2;\ \bullet HO_2 + H^+ + e^- \rightarrow H_2O_2 \tag{1}$$

$$H^+ + OH^- \rightarrow \bullet OH;\ \bullet OH^+\ \bullet OH \rightarrow H_2O_2 \tag{2}$$

Weaker nucleophile acetate can impact the functional groups of the cell membrane of the bacteria in low light conditions, and this allows the stored electron to be released and create superoxide or other ROS to kill the bacteria. As nitrate is not a strong nucleophile, it is able to strongly trap the electron at the lattice defect sites because of its low nucleophilicity. ZnO NPs were functionalized with 0, 1.5, 3, and 6% of polymeric fibers constructed of recycled polyethylene terephthalate (r-PET) from postconsumer water bottles. These fibers were created in order to test their effectiveness against germs and fungi [35]. In both the light and the dark, ZnO-Ac QDs exerted a stronger inhibitory effect [36]. In recent years, researchers have explored the impact of ZnO NPs in borosiloxane on *E. coli* bacteria development and growth. *E. coli*'s growth and development were unaffected by the presence of NPs in borosiloxane. The density of bacterial cultures cultivated on the composite was lowered by 58, 90, and 96% when ZnO NPs were added to the polymer at concentrations of 0.001, 0.010, and 0.10%, respectively. Bacteriostatic characteristics of aqueous colloidal solution of ZnO NPs were tested in another set of tests. Each of the concentrations investigated was 0.0001, 0.001, 0.01, and 0.10%. Nanoparticle doses of 0.001, 0.011, and 1.0% protected bacterial growth and development. The intensity of the bacterial culture is decreased by 93%, with a concentration of 0.0001% [37,38]. The ZnO NPs' ability to inhibit bacterial growth is proportional to their average particle size. ZnO NPs are proven to be more effective against bacterial activities at higher concentrations when their size is reduced [39].

**Table 1.** Antimicrobial properties of ZnO NPs.

| Product | Size (Nanometer) | Species of Bacteria | Mechanism | Ref. |
|---|---|---|---|---|
| ZnO NPs | 30 | *E. coli* | Damage the membrane's integrity and the production of ROS. | [40] |
| | 8 | *S. aureus, E. coli, and B. subtilis* | Due to the release of free $Zn^{2+}$ ions formed in the ZnO suspension for significant growth inhibition of bacteria. | [39] |
| | 10 | *L. Plantarum* | By reaction between the surface of ZnO and cell surface enzymes of bacteria | [41] |
| | 12, 45 | *E. coli* | ZnO involves disrupting the membrane of bacteria | [42] |
| | ∼20 | *E. coli* 11,634 | $H_2O_2$ generation | [43] |
| | | *S. aureus*, *E. coli* | Release of $Zn^{2+}$ ion | [44] |
| | ∼80 | *V. cholera* | Depolarization of the membrane structure, enhanced permeabilization, DNA damage, and ROS production | [45] |
| | 40 | *S. pyogenes* (MTCC1926), *S. mutans* (MTCC497), *S. flexneri* (MTCC1457), *V. cholerae* (MTCC3906), *S. typhi* (MTCC1252) | $Zn^{2+}$ release and ROS production | [46] |
| | 90–100 | enterotoxin *E. coli* (ETEC), *V. cholerae* | adenylyl cyclase function inhibition, cAMP levels are reduction | [47] |

**Table 1.** *Cont.*

| Product | Size (Nanometer) | Species of Bacteria | Mechanism | Ref. |
|---|---|---|---|---|
| Ag-ZnO nanocomposite | 64 | GFP *E. coli*, *S. aureus* | Release of $Ag^+$ and $Zn^{2+}$ and ROS production | [48] |
| Phβ-GBP-coated ZnO NPs (Phβ-GBP-ZnO NPs) | 20–50 | *P. vulgaris*, *S. aureus* | Changes in the permeability of bacterial cell membranes and a high quantity of reactive oxygen species (ROS) | [49] |
| ZnO nanocatalyst | ∼18 | *E. coli*, *B. subtilis*, *S. typhimurium*, *K. pneumonia* | $OH^-$, $H_2O_2$ generation, ROS generation | [50] |
| ZnO-CdO nanocomposite | 27 | *P. aeruginosa*, *E. coli*, *K. pneumonia*, *P. vulgaris*, *S. aureus*, *B.* spp. | Release $Cd^{2+}$ and $Zn^{2+}$ and generate ROS ($H_2O_2$, $OH^-$, and $O_2{}^{2-}$) | [51] |
| ZnO QDs | 4 | *C. metallidurans* CH34, *E. coli* MG1655 | Released $Zn^{2+}$ ion generated toxicity | [52] |
| Kaoline-ZnO nanocomposites | | *E. coli*, *S. aureus*, *P. aeruginosa*, *E. faecalis* | $Zn^{2+}$ release, subsequent diffusion of ions into cytoplasm | [53] |
| ZnO nanostructures (ZnO NSs) | 70–80 | *S. aureus*, *P. vulgaris*, *K. pneumoniae*, *S. typhimurium* | Damage to cell membranes by reactive oxygen species (ROS) | [54] |
| ZnO-Ge NPs | 20 | *E. faecalis*, *P. aeruginosa* | Bacterial cell death triggered by cell penetration | [55] |
| ZnO-SA composites | | *S. aureus*, *E. coli* | Reactive Oxygen Species production | [56] |
| ZnO@GA NPs | 11.5 ± 4.4 | *S. aureus*, *E. coli* | Due to GA's strong affinity for the bacterial cell membrane and the increased lipophilicity that results from its addition. | [57] |

Due to the small particle size and the large surface area, ZnO NPs show enhanced antimicrobial and antifungal activities [58]. ZnO NPs inhibited the growth of the plant pathogen *F. graminearum* [59]. Antifungal activity that has been found for ZnO NPs was effectively evaluated against *A. niger*, *P. expansum*, *A. alternata*, *B. cinerea*, and *F. oxysporum* [60]. It also showed great effectiveness against *E. salmonicolor*, which is a coffee fungus [61], *B. cinerea* [62] and *P. expansum* [63], and phytopathogenic fungi species; *Fusarium oxysporum f.sp. lycopersici* is a fungal plant pathogen. It is a big pathogen in the tomato plant. It has a violet-to-white color on most media but does not produce a pigment on King's B medium. It has been spread to tomato seeds by the hands of contaminated workers, such as *F. solani*, and *C. gloeosporioids* [64]. Thus, the ZnO QDs have promising antifungal activities (Table 2). Therefore, ZnO-based NPs are crucial for their applications as disinfectants and sterilizing agents in the biomedical and healthcare industries. Moreover, ZnO NPs may be promising for inhibiting fungi and pathogens in agriculture- and food-based industries.

**Table 2.** Applications of ZnO QDs against Fungi.

| Type of Device | Type of Fungi Inhibited | Reference |
|---|---|---|
| ZnO QDs | *B. cinerea*, *P. expansum* | [64] |
| | *A. saloni*, *S. rolfii* | [65] |
| | *R. stolonifera*, *A. nidulans*, *A. flavus*, *T. harzianum* | [66] |
| | *E. salmonicolor* | [61] |
| | *A. fumigatus*, *C. albicans* | [67] |
| | *R. stolonifera*, *P. expansum* | [68] |
| | *C. krusei* | [69] |
| Zn/Mg Oxide QDs | *A. niger*, *Paraconiothyrium sp.*, *P. oxalicum*, *P. maculans* | [70] |
| CS-LiA ZnO QDs | *C. albicans* | [71] |

## 4. Photocatalytic Applications

Major contaminants in textile dyeing wastewater include unfixed dyes and inorganic salts. Existing treatment techniques are ineffective and have limitations. Wastewater from textile dyeing processes is poorly treated and immediately released into the environment. Long-term dumping endangers the ecosystem [72]. The high photocatalytic activities of ZnO NPs for various azo dyes were likewise extremely high, indicating a promising use in organic pollution remediation [73]. Since they are non-toxic, low-cost, and much more effective at absorbing over a wide portion of the solar spectrum, ZnO nanostructures have been demonstrated to be promising photocatalyst candidates for application in photodegradation. The bandgap energy of ZnO is also a significant element in influencing its photocatalytic activity in use [74]. ZnO NPs degraded reactive orange (RO) and methylene blue (MB) (Figure 2) dyes under blacklight irradiation [75]. It also degraded methyl orange, methyl red, reactive blue 21 (RB-21) [76], and rhodamine B dye [77]. Moreover, modified ZnO NPs showed outstanding photocatalytic effects in the decomposition of methylene blue [78]. Manganese-doped ZnO NPs also exhibited excellent performance in the decomposition of methylene blue in the presence of UV and visible light [79]. Ce-doped ZnO NPs showed effective photocatalytic decomposition of harmful dyes, such as direct red-23(DR-23) under UV irradiation [80], direct blue-86 (DB-86), methyl orange (MO), and food black-2 (FB-2) dyes under ultraviolet and visible light irradiation [81]. ZnO-based MOF photocatalyst, ZnO@MOF-46(Zn), has been investigated for methylene blue (MB) degradation, which showed promising results in degrading more than 90% of the dyes (Figure 2) [82]. In a photocatalytic system, the catalyst's surface is where the photoinduced atomic or molecular change or reaction occurs. When a photocatalyst is excited by photons with energies that are equivalent to a level that is equal to or higher than its bandgap energy, electrons absorb the energy from the photons. Hole formation in the valance band (VB), which has the ability to produce hydroxide radicals, occurs when the energy level exceeds the bandgap energy level. It is possible for a hole to start a dye molecule's disintegration process by reacting with the target molecule, which causes the loss of one of the molecule's electrons. ZnO granules are only occasionally used in applications that offer UV protection due to the material's photocatalytic characteristics. A photocatalyst ZnO produces reactive free radicals when it is exposed to UV light. UV radiation energies, electrons in ZnO are ultimately responsible for producing electron-hole pairs (e-h) [73]. The photocatalytic properties of ZnO produced by thermal evaporation and chemical deposition, in UV-induced degradation of dyes, such as methyl orange, depended on the particle size, shape, and production method of ZnO. Modifying the ZnO photocatalysts' particle size, shape, and as well as the manufacturing conditions and methodologies, may result in an improvement in the overall effectiveness of the photocatalytic process [75]. Therefore, ZnO-based photocatalysts are highly efficient in the degradation of dyes in industrial effluent to protect the environment.

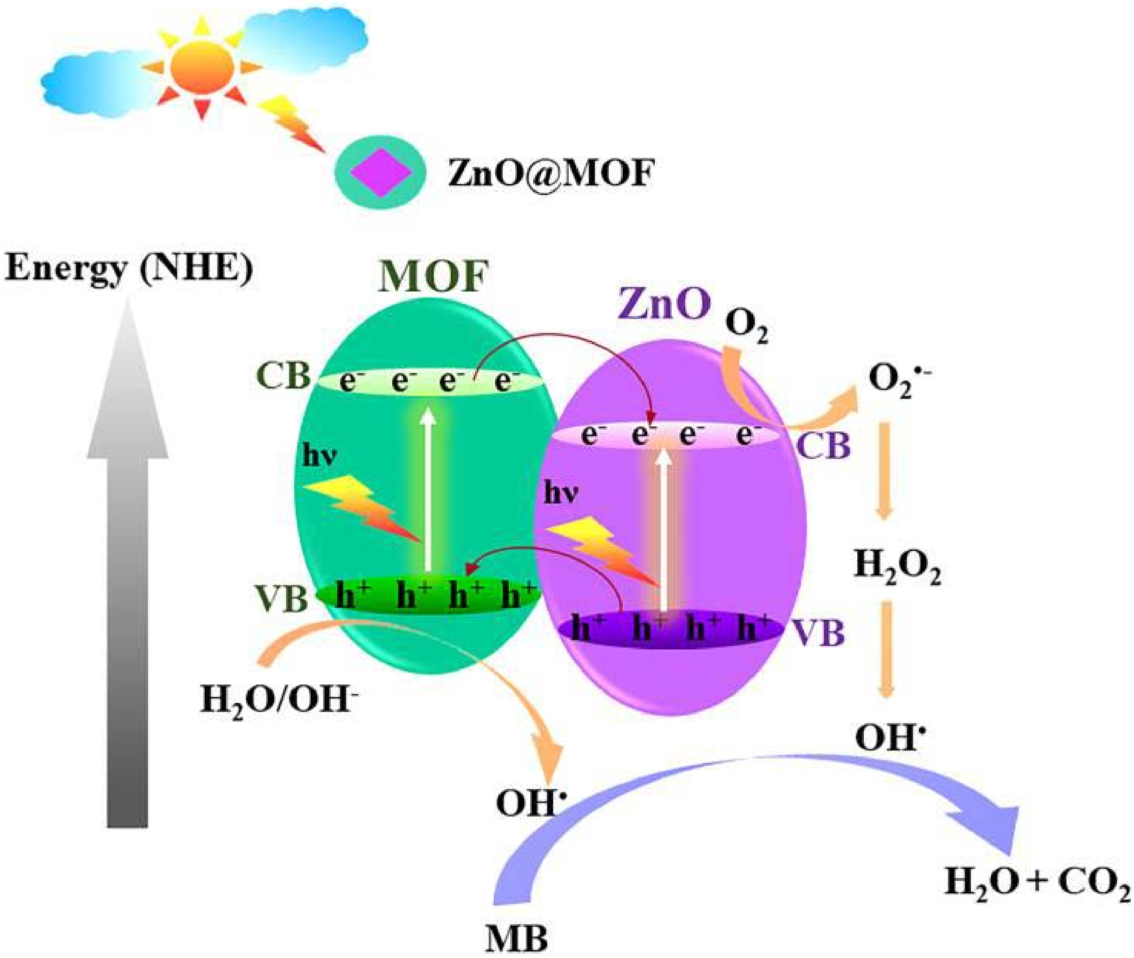


**Figure 2.** Photocatalytic mechanism of ZnO@MOF-46(Zn). Proposed reaction mechanism over ZnO@MOF-46(Zn) for photodegradation [82].

## 5. Biosensing Applications

Several ZnO NPs were used for sensing different biomolecules (Table 3). In electrochemical biosensor development, nanostructures of ZnO were used. Analytes, such as uric acid, cholesterol, dopamine, and DNA can all be distinguished using ZnO-based electrochemical biosensors [83–86]. With a high isoelectric point, ZnO can be used in electrochemical biosensors because it has high biocompatibility, a fast charge transfer property, and an easy and more grounded attachment of diverse proteins on its surface. The fluorescence and piezoelectric characteristics of ZnO make it a delicate optical and piezoelectric biosensor. A consistent and repeatable method of developing ZnO nanostructures directly on electrode surfaces is vital for biosensor innovation. To develop electrochemical biosensors for the sensing of biologically relevant analytes, such as DNA, metabolites, and cancer indicators, ZnO-based platforms can be employed as an immobilization matrix [87]. Acetylcholinesterase [88], glucose [89], xanthine [90], DNA [91], lactate [92], cholesterol [93–95], N-acyl homoserine lactone [96], uric acid [97], epinephrine [98], and urea [99] have all been shown to be successfully sensed by ZnO NPs. ZnO NPs-modified carbon paste electrode [100], ZnO NPs film [101], ZnO/chitosan-graft-poly(vinyl alcohol) core-shell nanocomposite [102] etc. are utilized to detect glucose. When constructing a hemoglobin biosensor, ZnO NPs–polypyrrole film has been used [103]. For the detection of acetylcholinesterase, ZnO nanocomposite ZnO NRs/NWs were produced and utilized [104].

**Table 3.** Applications of ZnO NPs in biosensing.

| ZnO NPs | Biological Compound Sensing | Ref. |
| --- | --- | --- |
| ZnO NRs/TNs | Acetylcholinesterase | [104] |
| ZnO/chitosan-graft-poly(vinyl alcohol)core-shell nanocomposite | Glucose | [102] |
| ZnO/chitosan/MCNT/polyaniline composite film | Xanthine | [90] |
| Ionic liquid/ZnO/chitosan/gold electrode | DNA | [91] |
| ZnO NPs decorated multi-walled carbon nanotubes (MWCNT) | Lactate | [92] |
| MWCNT–ZnO NPs | Cholesterol | [93] |
| Cysteamine functionalized ZnO NPs | N-Acyl Homoserine Lactone | [96] |
| Enzyme electrode modified by ZnO NPs | Uric Acid | [97] |
| ZnO nanoparticle/1, 3-dipropylimidazolium bromide ionic liquid-modified carbon paste electrode | Epinephrine | [98] |
| Nanostructured ZnO film for urea sensor. | Urea | [99] |

In the development of enzymatic biosensors, ZnO NPs are employed. A new L-lactate sensor has been created using an enzyme electrode customized with ZnO NPs and MWCNT [105]. Through electrostatic interaction, ZnO can immobilize elements with low isoelectric points [106,107]. As an example, MWCNT/ZnO nanofiber-based biosensors can be used to detect malarial parasites [93]. ZnO thin films are also ideal for biosensing systems that require extreme sensitivity while maintaining a low cost. These films were manufactured using a flexographic printing process, which resulted in a nanotextured surface. These surface nanostructures have excellent execution for increasing surface functionalization [108]. ZnO nanorods were grown hydrothermally, and ZnO thin films were deposited electrochemically. Furthermore, ZnO nanorods and thin films were also investigated for their potential use in chemical and biological sensing applications. In addition, a ZnO nanorod-based strontium ion sensor was created. ZnO nanorods showed better response than ZnO thin films. ZnO nanorods are advantageous because their surface area-to-volume ratio is much higher than that of ZnO thin films [109]. ZnO and nanowires (NWs) have been studied for use as sensors. Interest in III-nitride nanowires, such as GaN and AlN, increased their prospective applications. NWs' high surface-to-volume ratio should increase sensor sensitivity and selectivity. High-performance NW transistors can be used to build a generic sensing device. Attaching a recognition group to the nanowire's surface enables specialized sensing. An amide link between the amine group of APTES (3-Aminopropyl)triethoxysilane) and the carboxylic group in mercapto propionic acid (MPA) allows MPA to be immobilized on ZnO surfaces. APTES and ODTMS (octadecyltrimethoxysilane) monolayers can covalently functionalize hydroxylated GaN and AlN surfaces. Schiff-base selectively immobilizes label-free oligonucleotides. Fluorescence microscopy allowed base synthesis of APTES-functionalized III-nitride films and hybridization with a fluorescently tagged oligonucleotide [110]. cTnT (cardiac troponin T)-spiked human serum was detected by a ZnO nanostructured biosensor. ZnO electrodes and serum buffer charge distribution helped achieve excellent detection. Electrochemical imbalances from cTnT binding and polarization were revealed by electrochemical impedance spectroscopy and Mott–Schottky. Binding creates ZnO's space charge layer (SCL) and the electrolyte's Helmholtz layer. Label-free and sensitive methods can detect cTnT at 0.1 pg/mL. Multiplexed ZnO sensors detected cTnT and cTnI. Nonspecific and cross-reactive antibodies reacted with BSA and cardiac isoforms (-cTnT and -cTnI) [111].

Further, copper-doped ZnO NPs, $Cu_xZn_{1-x}O$ (where x is 0, 0.01, 0.02, 0.03, or 0.04), were utilized as a nonenzymatic electrochemical sensor to detect glucose [112]. Glucose sensing may be performed using pure ZnO and $Zn_{1-x}Co_xO$ (where x is 0.05, 0.10, or 0.15) NPs. With other interfering chemicals, such as uric acid, ascorbic acid, l-dopa, and hydrogen peroxide, the sensor preferentially oxidizes glucose [113]. An electrode constructed of glassy carbon (GC) that has been doped with Fe-doped ZnO nanoparticles (Fe@ZnO NPs) exhibited good glucose sensing capability electrochemically [114]. ZnO NPs may boost acetylcholinesterase activity and so increase the efficacy of enzyme electrodes [115]. ZnO NPs were evenly distributed in a chitosan matrix and utilized to build a hybrid nanocomposite coating over indium tin oxide to quantify cholesterol in blood samples [95]. Cholesterol oxidase (ChOx) mounted on ZnO nanoporous thin films developed on gold surfaces are sensitive to cholesterol detection [116]. Due to its high surface area, large excitation binding energy, wide band, nontoxicity, chemical stability, good biocompatibility, and high electron communication property, a nano-ZnO film was fabricated on indium tin oxide ITO using the sol-gel technique. This film was used to immobilize cholesterol oxidase (ChOx) [117]. Biosensors that are capable of identifying l-lactate and other biological and chemical species could be developed by using gold nanoparticles coated on ZnO nanorods as a suitable matrix. These biosensors well recognized the l-lactate [118]. The $MnAl_2O_4$ $ZnAl_2O_4$ NM/GCE/Nafion combination is a potential sensor probe for the specific diagnosis of 3-CP on a wide scale in healthcare domains [119]. Therefore, ZnO NP-based biosensors are attractive for their promising applications.

## 6. Bioimaging Applications

ZnO NPs have demonstrated remarkable promise in bioimaging owing to their superior biocompatibility and inexpensive cost. The UV-blue light emitted by ZnO NPs fabricated using the gas evaporation process is intense. Therefore, it is compatible for bio-conjugation and can be used for bioimaging [120]. The ZnO surface was capped with covalently bound $SiO_2$ and $TiO_2$ layers with a 0.5 nm capping thickness, resulting in strong PL emission in the visible region. There were strong bioimaging capabilities in plant cells. Due to their greater quantum yields than the fluorescein standard material, uncapped ZnO and ZnO with a $TiO_2$ cap were suitable for bioimaging applications [121]. Enhanced yellow emissive Gd-doped ZnO quantum dots, had less cytotoxicity and held promise for magnetic resonance imaging (MRI) [122]. ZnO@$Gd_2O_3$ multimodal hybrid nanostructures might be useful as contrast agents in T2-weighted MRI [123]. Doped ZnO exhibited improved CT (computerized tomography) imaging and MRI in vitro for great tissue penetration depth with high-resolution three-dimensional visual reconstruction due to its minimal toxicity in vivo [124]. Electrochemical investigation of ZnO NPs revealed it to be a safe alternative contrast medium for use in CT scanning [125]. Cu-doped ZnO NPs have the ability to be employed in positron emission tomography (PET) imaging studies of cancer [126]. Using silica-coated Ga(III)-doped ZnO: $Yb^{3+}$, $Tm^{3+}$ for near-infrared optical imaging is possible due to its low in vivo toxicity and ability to induce photon avalanche processes (OI) [127]. ZnO NPs are an innovative form of a viable material for fluorescence-based imaging. In order for ZnO fluorescence to take place, the ZnO bandgap has to be activated by UV light. Since ultraviolet light can only penetrate the skin a few millimeters deep, it cannot be used for the majority of in vivo research. It was proposed that ZnO NPs should be doped with magnetic elements in order to generate unique binary probes that are capable of fluorescence; magnetism would make it possible for MRI to detect tagged tissues even when they are located deep inside the body. Recent research has resulted in the development of $Fe_3O_4$@ZnO core-shell nanoparticles with the goal of transferring carcinoembryonic antigen (CEA) into dendritic cells (DCs) for the treatment of cancer in mice via immunotherapy. These $Fe_3O_4$@ZnO core-shell nanoparticles were efficient nanocarriers for antigen distribution, and they were also able to be identified by confocal laser scanning microscopy (CLSM) in vitro and MRI in vivo [111]. The ZnO.$Fe_3O_4$@ZnO Chitosan (CS) NPs have important biological applications. $Fe_3O_4$@ZnO CS NPs have been the subject of significant research for their possible utility in drug delivery, photocatalysis, magnetic separation, and other domains.

The anti-hepatocellular carcinoma effects of transferrin receptor-functionalized and DOX-loaded $Fe_3O_4$@ZnO nanocomposites were investigated. After X-ray irradiation,

$Fe_3O_4$@ZnO nanocomposites showed improved chemotherapeutic efficacy and radiosensitizer characteristics [124]. Two-photon emission from ZnO NPs can be distinguished from SHG (second harmonic generation) emission by linewidth, emission frequency relative to input light, and emission duration. Two-photon emission lasts longer than SHG emission. If the SHG signal emits light above the ZnO bandgap, weak autofluorescence may result. At 745 nm, when the pump laser's two-photon energy doubles and exceeds ZnO's bandgap, two-photon fluorescence can be observed alongside SHG. Two-photon fluorescence begins at 385 nm, near the ZnO band edge, and SHG at 372.5 nm. SHG was studied using zebrafish blood and a Ti:Sapphire laser. The author performed all tests at laser excitation wavelengths above 750 nm to rule out two-photon absorption. Blood from ZnO-injected zebrafish demonstrated enhanced thrombocyte uptake [125]. ZnO quantum dots (QDs) and nanocrystals are safer alternatives to other substances in this class. ZnO quantum dots have a high efficiency of UV-blue emission. As a direct consequence of this, ZnO nanocrystals represent an intriguing possibility for use in the area of bioimaging [126]. Thus, imaging modalities utilizing ZnO-based NPs are crucial for their promise in medicine and healthcare.

## 7. Gas Sensing Using ZnO

When it comes to biosensors and chemical sensors, ZnO is a fascinating substance because it can simultaneously detect changes in mass, field effect, and surface resistivity. This semiconducting metal oxide has the potential to be a multisensing sensor platform. ZnO NPs may be utilized as sensing systems for gas sensors because of their increased sensitivity and long-term durability [128]. ZnO NPs produced by annealing zinc carbonate hydroxide at 400 °C displayed outstanding $NO_2$ sensing properties. It takes 30 s to react to $NO_2$ and another 120 s for it to make a recovery [129]. At ambient temperatures, ZnO NPs produced from zinc hydroxide utilizing a trisodium citrate-assisted hydrothermal method showed a response to 5 ppm $NO_2$ gas. At 400 °C, it also demonstrated a strong response to CO, ethanol, and acetaldehyde [130]. It has been demonstrated that ZnO is a potential material for application in sensors. This semiconducting metal oxide offers application as a substrate for integrated multisensing sensors since it can simultaneously detect changes in field effect, surface resistivity, and mass. When ZnO NPs were exposed to oxygen, they reacted significantly more strongly than the films did. Additionally, selectivity tests were carried out against additional gases that can be found in the exhaust of vehicles or chimneys [128]. ZnO nanostructures having a porous network structure with oxygen vacancies, synthesized by electrospinning technique, resulted in a greater and faster sensitivity to acetone vapor, as well as superior selectivity. The sensitivity and selectivity of polyvinylpyrrolidone (PVP)-modified ZnO nanoparticle-based gas sensors for trimethylamine (TMA) are quite remarkable. The sensor has a reaction time of 10 s and a recovery time of 150 s [131]. Nanosized ZnO powder created using the sol-spray combustion process has highly sensitive gas sensing characteristics to ethanol, and it responds and recovers in 10 s and 40 s, respectively, for different concentrations [132]. Ag-doped ZnO NPs and $MoS_2$ nanosheets coated with ZnO NPs also display sensitivity to $C_2H_5OH$ [133]. At the optimal operation temperature of 150 °C, $In_2O_3$ hollow microtubes decorated with ZnO NPs produced from metal-organic frameworks (MOFs) demonstrated a significant gain in ozone gas sensing ability [134]. The detection features of doped ZnO NPs for n-butanol gas demonstrate a high-performance gas detecting capability at an operating temperature of 300 °C, including strong gas response, excellent response/recovery time, selectivity, stability, and repeatability [135]. RF magnetron sputtering has a low cost, can generate uniform films across a large surface area, and is easy to manage. The sputtering method can adjust the base pressure, substrate temperature, RF power, deposition duration, and target-to-substrate distance. These parameters optimize gas sensing sensitivity. Low sputtering power (100 W) and high substrate temperatures (300–400 °C) yield accurate ZnO growth outcomes. Recent studies have focused on determining the room-temperature gas reaction. So far, this operation cannot be performed at room temperature. This study investigated deposited films' gas sensing characteristics at 205 °C, managed parameters to speed up reaction and recovery. Researchers increased annealing temperature, adjusted deposition time and substrate, added doping materials, and executed synthesis to improve gas sensing characteristics [136]. The bandgaps and work functions of ZnO and $Fe_2O_3$ are quite different from one another, despite the fact that both of these materials are n-type semiconductors. At the point where the $Fe_2O_3$ core and the ZnO shell meet, a heterojunction can develop, which results in the formation of potential barriers. Since ZnO has a larger work function, the electrons in its Fermi level flow into the lower Fermi level of $Fe_2O_3$, and this process continues until the Fermi levels of both materials are equal. This process is repeated multiple times until the work functions of ZnO and $Fe_2O_3$ are equivalent to one another. After the requirement of equilibrium has been satisfied, an electron depletion layer begins to form at the interface of the heterojunction. The transmission of electrons is extremely important for the surface [137]. ZnO NPs demonstrate the potential for applications in gas sensors. Furthermore, the ZnO NPs-based semiconducting metal oxide offers a platform for integrated multisensing sensors.

## 8. Medicinal Applications of ZnO NPs

Lipid-coated ZnO NPs have potential and can be a novel photosensitizer for cancer detection. The photogeneration of short-chain carbon-centered free radicals is induced by lipid bilayer coating, indicating that surface chemistry is important for different kinds of photogenerated free radicals. ZnO semiconductors convert UV energy into visible light. This suggests bioimaging or a LED reporter. When ZnO creates ROS within cells, it can destroy tumor cells. Too many ROS disturb the cell cycle and increase the risk of apoptosis or autophagy. ROS can damage membranes, proteins, and DNA through lipid peroxidation [138]. ZnO QDs nanoprobes in vitro may be utilized as a fluoroprobe alternative for cancer cell targeting. An innovative nanoprobe based on ZnO for in vitro imaging as a sensitive bioassay is promising. ZnO is a versatile material that may be used in a wide variety of medicinal contexts thanks to the fact that it is nontoxic and biocompatible. ZnO is an environmentally friendly compound that has potential use in cancer diagnostics and live cell imaging. In this particular research endeavor, transferrin served as the tumor-targeting ligand, and a ZnO nanocrystal bioconjugate that was coated in silane and had an amino functional group was used for the ligand conjugation process. The capability of the nanoprobes to specifically target breast cancer cells was tested [139]. Due to their biocompatibility, excellent selectivity, increased cytotoxicity, and ease of production, ZnO NPs may be utilized as an anticancer therapy [140]. ZnO nanocomposites are likewise applied in theranostics and drug delivery systems (Figure 3). Various ZnO NPs, for example, ZnO-quercetin [141], $Fe_3O_4$@ZnO:$Er^{3+}$,$Yb^{3+}$@(β-CD) nanoparticles [142], ZnO@PNIPAM hybrid NPs [143], ZnO-gated porMOF-AS1411 [144], biopolymer K-carrageenan wrapped ZnO NPs [145], ZnO quantum dots-conjugated Au nanoparticle [146], ZnO-GO (graphene oxide) nanocomposites [147], chitosan/ZnO bionanocomposite [148], chitosan-encapsulated ZnO quantum dots [149], $Fe_3O_4$@ZnO@m$SiO_2$ nanocarrier [150], ZnO-gated hollow mesoporous silica [151], ZnO Quantum Dots-Doxorubicin NPs [152,153], ZnO-DOX@ZIF-8 Core-Shell NPs [154] etc. are utilized for effective drug delivery for different ailments. For example, β-CD-modified $Fe_3O_4$@ ZnO: $Er^{3+}$ and $Yb^{3+}$ nanocarriers are effective for antitumor drug delivery and microwave-triggered drug release; a ZnO-gated porphyrinic metal organic framework-based drug delivery system is efficient for targeted bimodal cancer therapy, and biopolymer K-carrageenan-wrapped ZnO NPs are excellent drug delivery vehicles for anti-MRSA (Methicillin-resistant Staphylococcus aureus) therapy [142,144,145]. Furthermore, ZnO quantum dots have shown promise as a multifunctional anticancer agent, and DOX-FA-ZnO NPs have been implicated in the effective treatment of breast cancer (Figure 3) [155–157]. As a result, ZnO-based NPs are efficient as anticancer and antibacterial drugs, as well as therapeutics for other diseases.

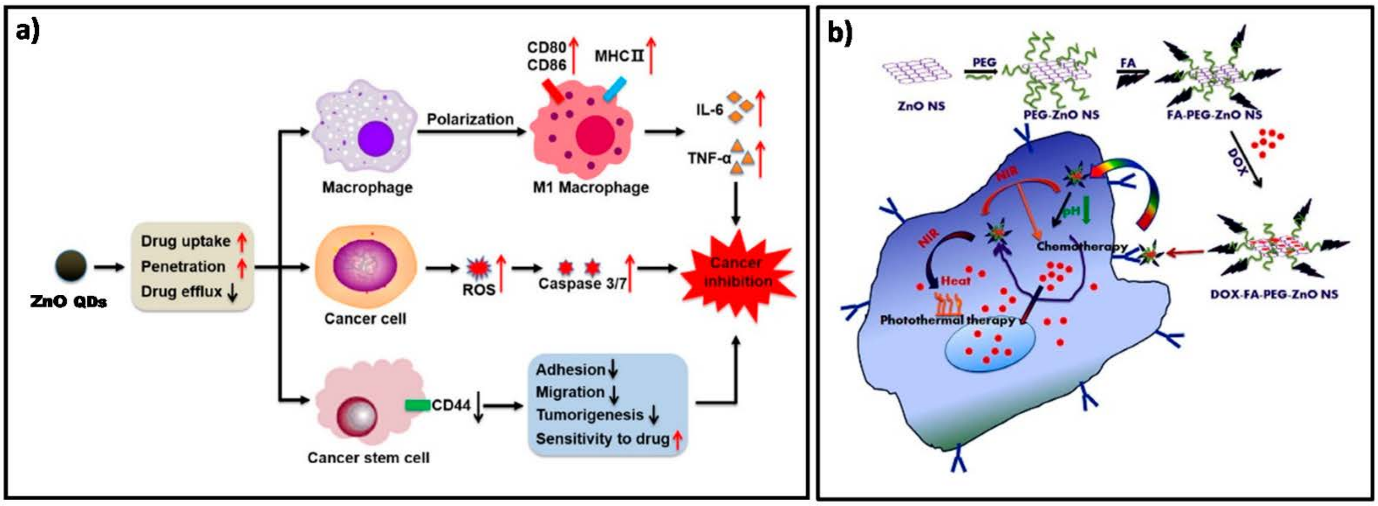


**Figure 3.** (**a**) Numerous antitumor effects of ZnO quantum dots as a multifunctional anticancer agent [156]. (**b**) Mechanism of action of DOX-FA-ZnO NPs in the treatment of breast cancer [157]. (Re-printed/adapted with permission from refs [156,157]).

## 9. ZnO in Food Industry

ZnO NPs have many prospective applications in food-based industries. ZnO NPs are potentially used in active packaging. Prior to the broad industrial use of nanoparticles in food packaging, it was essential to perform research on the regulatory concerns that must be addressed in light of the efficacy of NMs in protecting the chemical, physical, sensory, and microbiological quality of food. Modern packaging solutions that are lighter, more durable, and more practical may also substantially reduce shipping costs and environmental impacts [158]. ZnO nanoparticles included in polystyrene film or other suitable matrixes are suitable for several food packages and related uses [159]. ZnO NPs coated on PVC (polyvinyl chloride) films are examples of metal or metal oxide nanoparticles integrated in polymer nanocomposites, used as disinfectants, for food packaging, etc. [160]. Antimicrobial properties of a variety of metal and metal oxide NPs have been promising. Nanocomposite films composed of polystyrene, polyvinyl chloride, and polyvinylpyrrolidone have also been shown to bind to ZnO NPs and inactivate food pathogens [159]. Lactate in foods could be detected using an Au/NanoZnO/lactate dehydrogenase (LDH) bioelectrode biosensor [161]. The electrochemical biosensor based on ZnO nanowires has a lot of promise for detecting L-lactic acid in real samples [162]. ZnO NP has investigated several bacteria, the majority of which were foodborne pathogens. ZnO NP has been shown to be more effective than powder as an antibacterial agent in the food sector. The findings suggested that it might be employed as a food preservation agent. *Salmonella* species are widely suspected to be the primary pathogens responsible for many different types of food poisoning. The presence of *Salmonella* species has been confirmed, causing widespread alarm in the food service industry. *Staphylococcus* bacteria are another major cause of food poisoning. In immunocompromised people, it is most often connected with nosocomial infections but can also spread from person to person in the community. Within the genus *Staphylococcus*, the species *S. aureus* is regarded as the most significant. They live on the skins of people and other animals, but they rarely spread to other organs and cause diseases there. The potential of ZnO NP as an antibacterial agent, the majority of which are foodborne pathogens, has been perspective. Further, micrographs of *S. typhimurium* and *S. aureus* cells treated with ZnO NP were used to examine the effect at the cellular level [163]. Chitosan with ZnO NP-infused gallic acid films (CS-ZnO@gal) showed extraordinary antibacterial capability and great antioxidant activity when compared to pure chitosan, which may be explored for active food packaging applications [164]. ZnO NPs loaded on starch-coated polyethylene film were efficiently examined for their biocidal activity against model bacteria using killing kinetics and zone inhibition of bacterial growth.

Nano ZnO could disinfect food dyes and water-grown bacterial cultures. Thus, nano ZnO may be utilized to remove rapid green dye and bacterial toxins, such as *E. coli* and *B. subtilis*. Histology and cytology laboratories utilize quick green dye despite accusations that it may promote cancer, mutagenesis, and irritation. Furthermore, fast green dye is immunotoxic. Multiple efforts have been undertaken to remove this dangerous watercolor.

*B. subtilis* can cause allergic reactions, is prevalent everywhere, is conveyed by water, and can spread quickly. *E. coli* causes urethritis, gastroenteritis, and meningitis in infants [165]. As a consequence, the nano ZnO material has the opportunities to be utilized as a food packaging material to avoid food contamination due to micro-organisms. ZnO nanorods produced using the hydrothermal method also showed antibacterial activity. ZnO's performance against *E. coli* and *B. atrophaeus* was effective. Both species were found to have damaged cell membranes. Polyethylene-based films feature exceptional mechanical strength, hydrophobicity, and moisture barrier characteristics, which are some of the most crucial features of a high-quality packaging film and may be further improved by incorporating ZnO NPs [166]. Nanofiltration is a good technology for clarifying and concentrating raw juices, in which the elements are separated depending on their molecular size. ZnO NPs are often utilized in the construction of nanofibrous membranes or as filtration aids in food processing. ZnO NPs have been observed to significantly enhance the quality of pear juice by reducing cloudiness [167]. Thus, ZnO-based nano- and polymer composites have shown promising applications in the food industry to improve food quality.

## 10. Applications of ZnO in Environmental Industry

Outstanding photocatalytic activity was demonstrated by ZnO NPs generated from the microalgae chlorella in the destruction of the pollutant known as dibenzothiophene (DBT) [168]. The degradation of the organic pollutants, methyl orange and methyl blue, by $ZnFe_2O_4$/ZnO NPs has shown outstanding performance [169]. Metal oxide-based photocatalysts created from ZnO@$In_2O_3$ core-shell hollow tubes have the potential to speed up the degradation of organic dyes as well as antibiotics in wastewater [170]. ZnO NPs are among the semiconductor nanostructures that are investigated most frequently for environmental uses. This is because they have high photocatalytic activity. They have the potential to break down antimicrobial agents as well as organic contaminants found in water and air [171]. The ZnO nanocomposites have a high rate of textile effluent degradation. Nanocomposites of ZnO/CdO [172], ZnO/Ag [173], CuO-ZnO [174], CuAu–ZnO–graphene [175], and ZnO/zinc tin oxide nanocomposites (ZnO/ZTO) have demonstrated 50% photocatalytic degradation efficiency and 77% COD removal from textile wastewater when exposed to sunlight [176]. Photodegradation of rhodamine B (Figure 4), methylene blue, and neutral red may be utilized to clean wastewater using artemia eggshell-ZnO nanocomposites [177]. Hybrid Au/ZnO nanostructures may be utilized in water treatment for heterogeneous photocatalytic applications [178]. ZnO/$Fe_3O_4$-sepiolite nanostructured materials work well as a photocatalyst in water for pollutant removal [179]. The application of nano-ZnO as a remedy for water tainted with fast green dye has been shown to be effective [165]. ZnO NPs were able to inhibit the growth of waterborne pathogens, such as *E. coli*, *S. epidermidis*, *Proteus*, and *K. pneumoniae*, in municipal wastewater, demonstrating their enhanced antibacterial activity [180]. Inorganic UV blockers are semiconductor oxides, such as ZnO, $TiO_2$, $Al_2O_3$, and $SiO_2$. It has been established that nanosized titanium dioxide and ZnO are superior to larger sizes in both their capacity to absorb and scatter ultraviolet light as well as their efficacy in blocking UV radiation [181]. Coating a fabric with a nanoparticulate layer or covering the surface of the fabric with three-dimensional surface structures are important methods for making a fabric water-resistant. It has been demonstrated that ZnO NPs are capable of achieving antistatic characteristics [182]. The employment of NMs, particularly ZnO, displays higher photocatalytic activity in comparison to their bulk counterparts [183]. Therefore, ZnO-based NPs are suitable candidates for their significant applications in environmental industries.

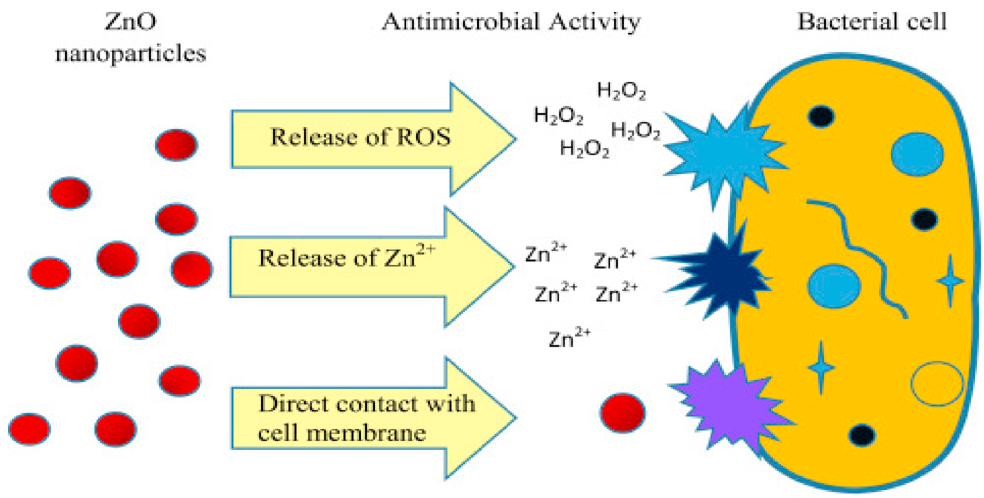


**Figure 4.** The mechanism of water disinfection by ZnO NPs [183].

## 11. ZnO in Cosmetics and Toiletries Industry

Using excisions of human skin placed in diffusion cells, it was possible to explore the skin absorption of ZnO NPs in a transparent sunscreen formulation. Only 0.03 percent of the zinc given to the epidermis was able to permeate into the receptor fluid under the skin. According to electron microscopy results, no ZnO NPs were discovered in the stratum corneum or in the viable epidermis of the mice. In vivo testing with human volunteers revealed that there was no substantial penetration of ZnO NPs into the skin. Skin surface ZnO NPs were found after application to the skin for 4 h and after removal from the skin. In skin folds and at the apex of hair follicle shafts, ZnO seemed to be restricted to a small area and did not spread to surrounding cells. At 24 h, no NPs were seen on the skin's surface, which was most likely due to washing the object. There was no indication of ZnO entering through the stratum corneum into the viable epidermis [184]. ZnO NPs are used in sunscreen. Nanosized ZnO cleans polluted regions due to their photocatalytic activity [185]. ZnO NPs/$Zn^{2+}$ are employed in a variety of eye makeup/eye shadow formulations [186]. ZnO NPs provide tremendous defense against sunburn caused by UV radiation and are proved to be safe [187]. There are many ZnO NM-based cosmetic products available in market, such as 'Proctor and gamble' manufacturers "Olay complete UV protective moisture lotion", 'Boots' manufacturers "Soltan facial sun defense cream", 'Image skincare' manufacturers "Solar defense organic moisturizer", 'Dermatone' manufactures "Moisturizing dermatone lips 'n' face protection crème", 'ColoreScience' manufacturers "Sunforgettable corrector colores SPF 20, sunforgettable SPF 30 brush range, wild to mild skin bronzer" [185]. Studies showed that four cosmetic products (commercial sunscreens) out of six contained ZnO NPs [188]. *Senna alata* methanol leaf extract ZnO NPs (SaZnO NPs) showed promising antibacterial properties in cold cream [189]. Adhatoda vasica leaf extract created with ZnO NPs showed promise in cold cream formulation. ZnO consumption is safe for cosmetic production. This chemical inhibits the bacteria's thiol peroxidases, glutathione reductases, and dehydrogenases, which kills them. ZnO destroys fungal hyphae and inhibits conidiophore growth. ZnO NPs are a cosmetic-friendly antioxidant. Its ability to permeate the stratum corneum protects against free radicals and other skin-damaging ROS. Particle size, degree of modification, and polydispersity of the mixture can further affect efficiency in their use in the cosmetic industry. Encapsulating vitamins, unsaturated fatty acids, and antioxidants in NPs makes them more stable and effective topically. ZnO NPs could improve healthcare and beauty. Their flexibility and small size make them promising cosmetic and dermatological tools. NPs will replace traditional preservatives in many cutting-edge cosmetics. The ZnO NPs are long-lasting, prevent disease-causing micro-organisms, and protect skin from UV rays [190]. In addition, ZnO NPs are also used in mouthwash, toothpaste, and root canal flings [191]. Studies are also investigating their toxicity in humans. Another study found that mouthwash comprising Ag/ZnO, 10 milligrams of NPs, and 100 mL of base material has the best antibacterial activity against *S. mutans* and is safe for cells; therefore, it may be used as an alternate mouthwash to chlorhexidine 0.2 percent in plaque control following *in vivo* testing. Over-the-counter mouthwashes can have cationic, anionic, or nonionic active components, all of which are known to affect bacterial membrane function. Chlorhexidine, $Cu^{2+}$, $Zn^{2+}$, and $Sn^{2+}$ are some of the most commonly used cationic components. It is well established that metal ions can affect bacterial membrane function and enzyme activity. It has been shown that zinc chloride mouthwashes are antibacterially active against Streptococcus bacteria, and that ZnO nanoparticles are active against *E. coli*. Therefore, it is clear that modified zinc salts and their derivatives are effective at preventing plaque. ZnO NPs are commonly found in sunscreen creams and act as both a nutritional supplement and a protective ingredient against UVA and UVB rays. There is conclusive evidence that silver and zinc NPs kill *S. mutans* bacteria while being almost entirely nontoxic to humans [192]. Therefore, ZnO NPs could easily be employed in cosmetic fabrication, including soap, face wash, hand wash, and many other cosmetic and toiletry industries. However, industries must evaluate the toxicity profile of ZnO-based products implicated in various cosmetic products for daily life use.

## 12. Applications of ZnO in Oil and Gas Industry

ZnO NPs with a high surface tension are able to lower the interfacial tension between water and oil in the context of increased oil recovery. Nano-enhanced oil recovery has attracted a lot of attention since modern NPs have substantial interfacial properties that can be used to adjust capillary forces in favor of easily accessing oil. Since ZnO NPs can lower interfacial tension, they have drawn attention as a possible tool for improving oil recovery. Nanostructured ZnO has tremendous adsorption capacity, a low growth temperature, excellent chemical stability, and high catalytic effectiveness, making it a promising material for increased oil recovery (EOR). The increased surface area makes it suitable for use as a catalytic agent. More specifically, this phenomenon would result in increased catalytic activity. The material's structure and synthesis process could be modified to alter its chemical and physical properties [193]. ZnO NPs with sizes ranging from 14 to 25 nm are effective scavengers for eliminating $H_2S$ and soluble sulfides from drilling fluids. Due to the higher performance of NPs in the elimination of $H_2S$, the usage of bulk ZnO will be reduced, resulting in less pollution in the environment and less use of nature's resources [194]. Microwave-synthesized ZnO NP claims to be a good candidate to be applied as an enhanced oil recovery agent [195]. To improve the repeatability of the $H_2S$ gas sensor, thermal evaporation and spray pyrolysis techniques were used to produce ZnO NPs coated with chromium (III) oxide ($Cr_2O_3$). The ZnO nanoparticle improved the responsiveness at high concentrations without altering the operating temperature, according to gas sensing studies [196]. In-doped ZnO nanoparticles showed better gas sensitivity towards volatile organic compounds (VOCs), acetone, benzene, ethyl alcohol, xylene, and toluene than undoped ZnO NPs [197]. As sensing materials, reduced graphene oxide-ZnO NPs (ZnO-rGO) hybrids were used to create an $NO_2$ gas sensor. Most significantly, the sensor has greater sensitivity, faster reaction time, and faster recovery time than a sensor based on rGO, suggesting that adding ZnO NPs to the rGO matrix improved the sensing performance for $NO_2$ sensing at ambient temperatures [198]. Dopped ZnO NMs showed better sensitivity towards VOCs, such as acetone, benzene, ethyl alcohol, xylene, and toluene, than undoped ZnO NPs [199]. Oil and gas firms must understand their water consumption, the demands and constraints of their operational sites, and the possibilities of investing in nanomaterial research to preserve and boost future profitability. While using steam-assisted gravity drainage (SAG), ZnO NPs may reduce viscosity and enhance heavy oil recovery while lowering the ratio of water to oil (WCUT %). The catalytic chemical reaction of NPs cracking carbon-sulfur bonds is assumed to be the root cause of lower viscosity. The lowest nanoparticle concentration lowers viscosity the most (0.2–0.5 percent wt). The viscosity reduction characteristics of ZnO NPs have a lower residual oil saturation (SOR) and WCUT percent [200]. The gas hydrogen sulfide is very corrosive, poisonous, and hazardous. During the drilling of gas and oil wells, it may seep into drilling fluid from rock formations. To limit pollution, preserve drilling employees' health, and avoid pipeline and equipment corrosion, $H_2S$ should be eliminated from the mud. The following chemical process was used to extract $H_2S$ from water-based drilling fluid using 14–25 nm ZnO with 44–56 $m^2$ per gram of specific surface area.

$$ZnO + H_2S \rightarrow ZnS + H_2O$$

In approximately 15 min, synthesized ZnO NPs can entirely remove $H_2S$ from water-based drilling mud, but bulk ZnO may take up to 90 min to eliminate 2.5 percent $H_2S$ [194]. ZnO NPs have a lot of promise for reducing viscosity since they can change wettability to water and wet through thick oil. However, after the addition of ZnO NPs, the surface tension decreased, reducing capillary forces and raising the relative permeability of the oil, which ultimately overpowered the gravitational forces to remove the oil. The initial amount of oil in place, or OOIP, was zero because the carbonate core was oily and wet. The results for sandstone core recovery ranged from 17.3 to 2 and 15% OOIP without NPs then to 20.68, 17.57, and 36.2% OOIP with NPs, respectively [201]. Bacteria that degrade petroleum are perhaps observed in Kuwait's and Bahrain's oil fields. Isolated bacteria are a potential bioaugmentation of petroleum-contaminated Arabian Gulf soils as well as biosurfactant manufacturing because of their numerous traits (crude oil breakdown and biosurfactant production). The biodegradation process may be slowed down by ZnO NPs. NPs have a significant influence on environmental micro-organisms' ability to develop and degrade. Some bacteria may be able to degrade crude oil without producing biosurfactants [202]. Thus, ZnO NPs are highly promising due to their crucial applications in the oil and gas industries, including viscosity reducers, inhibition of biodegradation, removal of the poisonous gas $H_2S$, and as gas sensors.

## 13. ZnO in Electronics Industry

Using ZnO NPs for light control, transparent and flexible $C_2H_5OH$ gas sensors can be created for wearable devices. The ability to detect dirty, toxic, and combustible gases is a key characteristic of today's wearable electronic devices. Semiconducting metal oxide nanostructures, such as ZnO nanorods, are attractive possibilities for highly sensitive and reliable gas sensors due to their high surface-to-volume ratio. Wearable electronics require gas sensors that are flexible, transparent, and operable at room temperature, however, conventional gas sensors do not meet these criteria. As a result, it is both an exciting and hard task to create a new generation of gas sensors that are able to run at room temperature while remaining flexible and transparent [203,204]. ZnO NPs can be utilized in dye-sensitized solar cells [205]. Organic compounds incorporating ZnO NPs have a significant potential for supercapacitors [206]. High-performance supercapacitor electrodes created from graphene-ZnO (G-ZnO) nanocomposite hybrid materials are promising [207]. In comparison with the pure graphene electrode, the graphene/ZnO nanocomposite electrodes showed enhanced electrochemical performance as a capacitor [208]. PVA/ZnO nanocomposite exhibited a modification in the dielectric constant, thus, its capacitance is widely used for device applications [209]. ZnO-loaded porous carbons (CMK-3 or CMK-8) are produced as a new anode component for lithium-ion batteries (LIBs) and have superior electrochemical characteristics than pure ZnO particles [210]. ZnO@NC@CNT showed high potentiality as an anode in Li-ion batteries for its high specific capacity, excellent rate capability, and cycling stability [211]. The capacity, rate performance, and cycling behavior of ZnO nanorods/reduced graphene oxide (ZnO/RGO) composite as an anode for sodium-ion batteries (SIBs) are significantly greater than those of pure ZnO substances [212]. Nanoparticle-based thin film transistors (TFT) display nonvolatile memory features, such as a conductance ratio of more than $10^5$, making them ideal for applications, such as data storage. Due to the voltage-controlled trapping and release of positive charges at the rough semiconductor/dielectric interface, there is a memory effect. More than 6 months of shelf life and useful endurance features are provided by the memory transistors operating in ambient air [213]. ZnO ink has the potential to be used in flexible printed electronics, which is a growing sector. Even at a relatively low processing temperature of 250 °C, the ZnO TFTs (thin film transistors) created from the suggested ZnO mixture ink showed considerably increased field effect mobility of 1.75 $cm^2\ V^{-1}\ s^{-1}$ and an on/off ratio of $5.89 \times 10^8$. The impact of ZnO NPs' incorporation into the thin film nanostructure on the structural, chemical, and electrical features of ZnO TFTs was investigated using a variety of structural studies [214]. ZnO NPs may also be applied to memory devices (Figure 5). Memory devices developed employing ZnO NPs encapsulated in a polystyrene layer exhibited promise for applications in write-once-read-many-times (WORM) memories [215,216]. ITO/PVP:ZnO/Al device constructed using ZnO has a higher on/off current ratio and better memory performance than the ITO/PVP/Al device (Figure 5) [217]. Figure 5 displays a comparison between the energy level diagrams of the PVP-based device and that of the ITO/PVP:ZnO/Al device and the mechanism of enhanced memory performance in the ITO/PVP:ZnO/Al device. Additionally, $Zn_{1-x}Cu_xO$ particles exhibit great potential to be employed in microwave semiconductor devices. Due to its remarkable ferroelectric, photoelectric, piezoelectric, catalytic, and dielectric qualities, ZnO is a semiconductor material that is both environmentally safe and highly desirable for usage in a wide variety of microelectronics applications. Numerous studies have focused on ZnO NPs because of their potential uses in the electronic field, such as luminescence, photodetection, gas sensors, and metal oxide semiconductors (MOS). Scientists in the field of semiconductor-based microelectronics have been interested in ZnO NPs due to their unique dielectric properties. Efforts are currently being made to improve these characteristics so that the materials can be used in microelectronics [218]. Accordingly, ZnO NPs are promising for the development of next-generation smart wearables and memory devices.

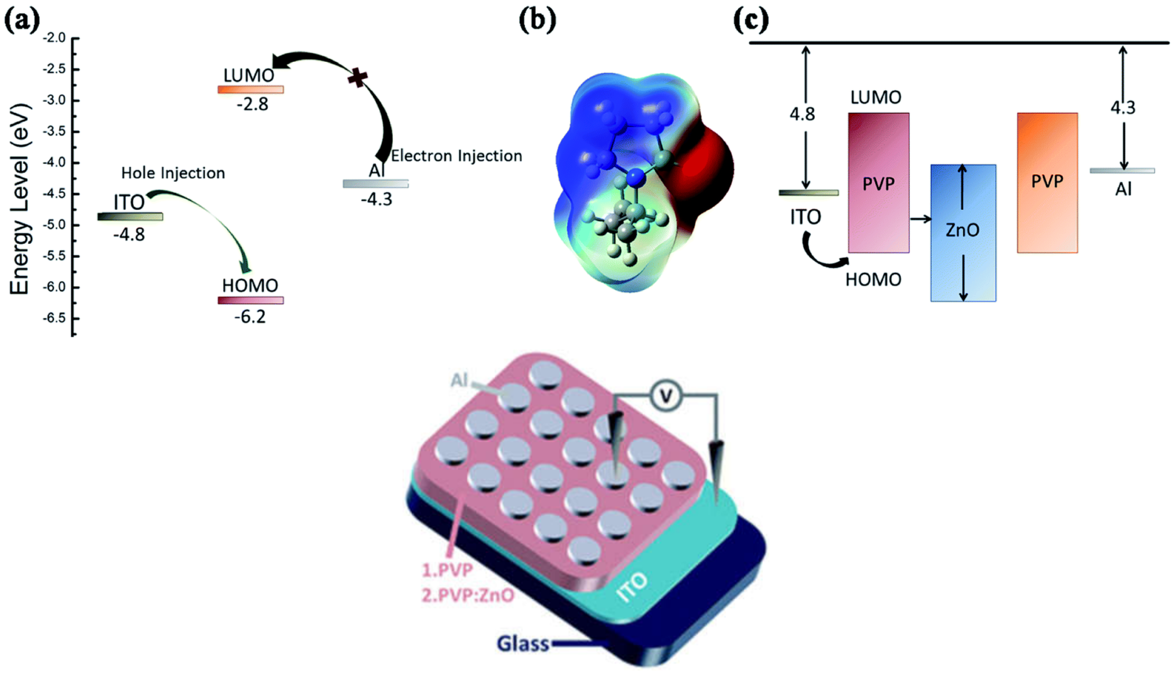


(**d**)

**Figure 5.** (**a**) Energy level diagram of the devices that are based on PVP. (**b**) The electrostatic potential (ESP) of the molecule as determined using DFT. (**c**) Illustration of the energy bands of the ITO/PVP:ZnO/Al device. (**d**) Schematic structure of resistive random-access memory (RRAM) device based on polyvinylpyrrolidone (PVP) and PVP:PVP:zinc oxide nanoparticle (ZnO NP) active layers [217].

## 14. Conclusions

ZnO NMs have vast applications in various sectors. Industry uses ZnO NMs to advance the products that are delivered to customers. These ZnO NMs have great antibacterial function, in degradation of organic pollutants and air pollutants, in gas sensing, and in solar cells. Some of these NMs can purify both wastewater and groundwater. ZnO NPs demonstrate free radical scavenging activity by efficiently donating electrons to highly reactive free radicals, indicating their potential for application as antioxidants. Due to the antioxidant and antibacterial properties of ZnO NPs, they are useful for tissue regeneration, and as sterilizers and disinfectants. In the food industry, ZnO NPs are utilized profoundly in packaging to avoid food contamination due to micro-organisms, inhibiting foodborne pathogens, and may be used as food preservative agents. These NMs are also used in biosensors, for glucose metabolism and homeostasis, accelerating insulin secretion, etc. ZnO NPs are effective in biological fluorescent imaging and are efficient and safe contrast agents in CT, PET, and MRI. ZnO-based NPs are prospective anticancer agents, novel antibacterial drugs, drug delivery platforms, and theranostic agents. ZnO NPs are promising for their applications in the cosmetic industry as skin care and UV-protectors, the oil and gas industries as purifiers and antimicrobial agents, and the electronic industry as gas sensors for wearable devices and memory devices. Finally, utilization of ZnO NPs has shown great prospect and promise in a wide range of industrial applications.

## 15. Future Perspectives

Metal oxide NPs, such as ZnO, have gained popularity as a way to treat antibiotic-resistant bacteria. ZnO NPs' many features are helpful for treating fatal infections [219,220]. It has been suggested that the green method, which involves obtaining NPs from a plant source rather than a chemical or physical one, is more cost-effective and less harmful to the environment. Significant in vitro antioxidant and free radical scavenging capabilities were also seen in ZnO NPs produced through the green technique employing plant extracts. Furthermore, synthetic routes may be expanded to include ZnO NPs sourced from a wide range of medicinal plants for biomedical applications [221–224]. As a result, more innovative green synthetic approaches may be helpful for fabricating highly efficient ZnO NPs for different industrial manufacturing applications.

The capacity of ZnO NPs to suppress microbial growth relies on their ability to form reactive oxygen species, which can damage biomolecules, release cations, interact with membranes, and deplete ATP. To enhance the effectiveness of novel ZnO-based NPs in inhibiting microbial growth with a suitable toxicity profile and to prevent microbial resistance, further studies are required [225,226]. ZnO NPs are involved in the production and secretion of insulin, as well as glucose metabolism and homeostasis; further investigation may be helpful in utilizing ZnO as a prospective insulin mimetic agent and enhanced mediator of glucose homeostasis. ZnO NPs are promising as anticancer agents, drug delivery systems, and theranostic agents. Thus, the development of novel ZnO-based NPs will further accelerate their use in medicine, tumor targeting, tumor imaging, and diagnosis.

Research on the use of nanostructures as agrochemicals (fertilizers or insecticides) to foster plant growth and protect crops is ongoing using ZnO NPs, with good prospects for ZnO NPs in agroeconomics. There has been a growing focus in recent funding and planned research on creating environmentally friendly ZnO NMs for effective solutions. Research on the use of ZnO in farming is quickly progressing. To ensure the safe use of nanoscale agrochemicals, regulatory frameworks must be established, and for this to happen, knowledge of how nanofertilizers function is crucial [227,228].

Applications of ZnO-based NPs are highly effective in electronic industries. Further investigations may reveal more state-of-the-art electronic devices and high-performance memory devices. Thus, the implications of ZnO NPs' use in different industrial settings are highly prospective and innovative as well.

**Author Contributions:** M.A.S. conceived the idea of research, contributed in preparing the manuscript, and revised it. N.N. contribute in manuscript preparation and revision. K.P.C. contributed in manuscript preparation. M.A.S. coordinated the whole study. All authors have read and agreed to the published version of the manuscript.

**Funding:** No external funding was received for this study. The APC was fully waived by the journal.

**Data Availability Statement:** Supplementary data is available, permissions.

**Conflicts of Interest:** The authors declare no conflict of interest.

## References

1. Tamirat, Y. The role of nanotechnology in semiconductor industry: Review article. *J. Mater. Sci. Nanotechnol.* **2017**, *5*, 202.
2. Sobolev, K.; Gutiérrez, M.F. How nanotechnology can change the concrete world. *Am. Ceram. Soc. Bull.* **2005**, *84*, 14.
3. Zhu, W.; Bartos, P.J.; Porro, A. Application of nanotechnology in construction. *Mater. Struct.* **2004**, *37*, 649–658. [CrossRef]
4. Havancsak, K. Nanotechnology at present and its promise for the future. In *Materials Science Forum*; Trans Tech Publications Ltd.: Wollerau, Switzerland, 2003; Volume 414, pp. 85–94.
5. Khan, I.; Saeed, K.; Khan, I. NPs: Properties, applications and toxicities. *Arab. J. Chem.* **2019**, *12*, 908–931. [CrossRef]
6. Natsuki, J.; Natsuki, T.; Hashimoto, Y. A review of silver NPs: Synthesis methods, properties and applications. *Int. J. Mater. Sci. Appl.* **2015**, *4*, 325–332.
7. Mohan, A.C.; Renjanadevi, B. Preparation of ZnO NPs and its characterization using scanning electron microscopy (SEM) and X-ray diffraction (XRD). *Procedia Technol.* **2016**, *24*, 761–766. [CrossRef]
8. Kalpana, V.N.; Devi Rajeswari, V. A review on green synthesis, biomedical applications, and toxicity studies of ZnO NPs. *Bioinorg. Chem. Appl.* **2018**, *2018*, 3569758. [CrossRef]
9. Bala, N.; Saha, S.; Chakraborty, M.; Maiti, M.; Das, S.; Basu, R.; Nandy, P. Green synthesis of ZnO NPs using Hibiscus subdariffa leaf extract: Effect of temperature on synthesis, anti-bacterial activity and anti-diabetic activity. *RSC Adv.* **2015**, *5*, 4993–5003. [CrossRef]
10. Matinise, N.; Fuku, X.G.; Kaviyarasu, K.; Mayedwa, N.; Maaza, M.J.A.S.S. ZnO NPs via Moringa oleifera green synthesis: Physical properties & mechanism of formation. *Appl. Surf. Sci.* **2017**, *406*, 339–347.
11. Aminuzzaman, M.; Ying, L.P.; Goh, W.S.; Watanabe, A. Green synthesis of ZnO NPs using aqueous extract of Garcinia mangostana fruit pericarp and their photocatalytic activity. *Bull. Mater. Sci.* **2018**, *41*, 50. [CrossRef]
12. Kumar, B.; Smita, K.; Cumbal, L.; Debut, A. Green approach for fabrication and applications of ZnO NPs. *Bioinorg. Chem. Appl.* **2014**, *2014*, 523869. [CrossRef] [PubMed]
13. Wong, K.K.; Ng, A.; Chen, X.Y.; Ng, Y.H.; Leung, Y.H.; Ho, K.H.; Djurišić, A.B.; Ng, A.M.C.; Chan, W.K.; Yu, L.; et al. Effect of ZnO nanoparticle properties on dye-sensitized solar cell performance. *ACS Appl. Mater. Interfaces* **2012**, *4*, 1254–1261. [CrossRef] [PubMed]
14. Middya, S.; Layek, A.; Dey, A.; Ray, P.P. Morphological impact of ZnO nanoparticle on MEHPPV: ZnO based hybrid solar cell. *J. Mater. Sci. Mater. Electron.* **2013**, *24*, 4621–4629. [CrossRef]
15. Udawatte, N.; Lee, M.; Kim, J.; Lee, D. Well-defined Au/ZnO nanoparticle composites exhibiting enhanced photocatalytic activities. *ACS Appl. Mater. Interfaces* **2011**, *3*, 4531–4538. [CrossRef] [PubMed]
16. Subhan, M.A.; Saha, P.C.; Rahman, M.M.; Akand, M.A.R.; Asiri, A.M.; Al-Mamun, M. Enhanced photocatalytic activity and chemical sensor development based on ternary B2O3 center dot Zn6Al2O9 center dot ZnO NMs for environmental safety. *New J. Chem.* **2017**, *41*, 7220–7231. [CrossRef]
17. Naveed Ul Haq, A.; Nadhman, A.; Ullah, I.; Mustafa, G.; Yasinzai, M.; Khan, I. Synthesis approaches of ZnO NPs: The dilemma of ecotoxicity. *J. Nanomater.* **2017**, *2017*, 8510342. [CrossRef]
18. Hanley, C.; Thurber, A.; Hanna, C.; Punnoose, A.; Zhang, J.; Wingett, D.G. The influences of cell type and ZnO nanoparticle size on immune cell cytotoxicity and cytokine induction. *Nanoscale Res. Lett.* **2009**, *4*, 1409–1420. [CrossRef]
19. Supraja, N.; Prasad, T.N.V.K.V.; Krishna, T.G.; David, E. Synthesis, characterization, and evaluation of the antimicrobial efficacy of Boswellia ovalifoliolata stem bark-extract-mediated ZnO NPs. *Appl. Nanosci.* **2016**, *6*, 581–590. [CrossRef]
20. Espitia, P.J.P.; Otoni, C.G.; Soares, N.F.F. ZnO NPs for food packaging applications. In *Antimicrobial Food Packaging*; Academic Press: Cambridge, MA, USA, 2016; pp. 425–431.
21. Kamaraj, P.; Sridharan, M.; Arockiaselvi, J.; Pushpamalini, T.; Vivekanand, P.A. Low cost synthesis of ZnO NPs and evaluation of their photocatalytic activity. *Mater. Today Proc.* **2021**, *36*, 873–877. [CrossRef]
22. Gandhi, S.; Kaur, R.; Sharma, V.; Mandal, S.K. Effect of calcination temperature on the morphology and catalytic properties of ZnO nanostructures fabricated from a chiral precursor for photodegradation of both cationic and anionic dyes. *New J. Chem.* **2022**, *46*, 3645–3657. [CrossRef]
23. Sundrarajan, M.; Ambika, S.; Bharathi, K. Plant-extract mediated synthesis of ZnO NPs using *Pongamia pinnata* and their activity against pathogenic bacteria. *Adv. Powder Technol.* **2015**, *26*, 1294–1299. [CrossRef]
24. Karnan, T.; Selvakumar, S.A.S. Biosynthesis of ZnO NPs using rambutan (*Nephelium lappaceum* L.) peel extract and their photocatalytic activity on methyl orange dye. *J. Mol. Struct.* **2016**, *1125*, 358–365. [CrossRef]

25. Ameen, F.; Dawoud, T.; AlNadhari, S. Ecofriendly and low-cost synthesis of ZnO NPs from *Acremonium potronii* for the photocatalytic degradation of azo dyes. *Environ. Res.* **2021**, *202*, 111700. [CrossRef]
26. Muthayya, S.; Sugimoto, J.D.; Montgomery, S.; Maberly, G.F. An overview of global rice production, supply, trade, and consumption. *Ann. N. Y. Acad. Sci.* **2014**, *1324*, 7–14. [CrossRef]
27. Ahmadpour, G.; Nilforoushan, M.R.; Boroujeny, B.S.; Tayebi, M.; Jesmani, S.M. Effect of substrate surface treatment on the hydrothermal synthesis of ZnO nanostructures. *Ceram. Int.* **2022**, *48*, 2323–2329. [CrossRef]
28. Jumina, J.; Mutmainah, M.; Purwono, B.; Kurniawan, Y.S.; Syah, Y.M. Antibacterial and antifungal activity of three monosaccharide monomyristate derivatives. *Molecules* **2019**, *24*, 3692. [CrossRef]
29. Guo, B.L.; Han, P.; Guo, L.C.; Cao, Y.Q.; Li, A.D.; Kong, J.Z.; Zhai, H.F.; Wu, D. The antibacterial activity of Ta-doped ZnO NPs. *Nanoscale Res. Lett.* **2015**, *10*, 336. [CrossRef]
30. Zhang, L.; Jiang, Y.; Ding, Y.; Daskalakis, N.; Jeuken, L.; Povey, M.; O'neill, A.J.; York, D.W. Mechanistic investigation into antibacterial behaviour of suspensions of ZnO NPs against *E. coli*. *J. Nanoparticle Res.* **2010**, *12*, 1625–1636. [CrossRef]
31. Da Silva, B.L.; Caetano, B.L.; Chiari-Andréo, B.G.; Pietro, R.C.L.R.; Chiavacci, L.A. Increased antibacterial activity of ZnO NPs: Influence of size and surface modification. *Colloids Surf. B Biointerfaces* **2019**, *177*, 440–447. [CrossRef]
32. Gudkov, S.V.; Burmistrov, D.E.; Serov, D.A.; Rebezov, M.B.; Semenova, A.A.; Lisitsyn, A.B. A Mini Review of Antibacterial properties of ZnO NPs. *Front. Phys.* **2021**, *9*, 641481. [CrossRef]
33. Sharma, D.; Rajput, J.; Kaith, B.S.; Kaur, M.; Sharma, S. Synthesis of ZnO NPs and study of their antibacterial and antifungal properties. *Thin Solid Film.* **2010**, *519*, 1224–1229. [CrossRef]
34. Sirelkhatim, A.; Mahmud, S.; Seeni, A.; Kaus, N.H.M.; Ann, L.C.; Bakhori, S.K.M.; Hasan, H.; Mohamad, D. Review on ZnO NPs: Antibacterial activity and toxicity mechanism. *Nano-Micro Lett.* **2015**, *7*, 219–242. [CrossRef] [PubMed]
35. Vázquez, K.; Vanegas, P.; Cruzat, C.; Novoa, N.; Arrué, R.; Vanegas, E. Antibacterial and Antifungal Properties of Electrospun Recycled PET Polymeric Fibers Functionalized with ZnO NPs. *Polymers* **2021**, *13*, 3763. [CrossRef]
36. Singh, T.A.; Sharma, A.; Tejwan, N.; Ghosh, N.; Das, J.; Sil, P.C. A state of the art review on the synthesis, antibacterial, antioxidant, antidiabetic and tissue regeneration activities of ZnO NPs. *Adv. Colloid Interface Sci.* **2021**, *295*, 102495. [CrossRef] [PubMed]
37. Chausov, D.N.; Burmistrov, D.E.; Kurilov, A.D.; Bunkin, N.F.; Astashev, M.E.; Simakin, A.V.; Vedunova, M.V.; Gudkov, S.V. New Organosilicon Composite Based on Borosiloxane and Zinc Oxide Nanoparticles Inhibits Bacterial Growth, but Does Not Have a Toxic Effect on the Development of Animal Eukaryotic Cells. *Materials* **2021**, *14*, 6281. [CrossRef]
38. Shi, L.E.; Li, Z.H.; Zheng, W.; Zhao, Y.F.; Jin, Y.F.; Tang, Z.X. Synthesis, antibacterial activity, antibacterial mechanism and food applications of ZnO NPs: A review. *Food Addit. Contam. Part A* **2014**, *31*, 173–186. [CrossRef] [PubMed]
39. Raghupathi, K.R.; Koodali, R.T.; Manna, A.C. Size-dependent bacterial growth inhibition and mechanism of antibacterial activity of ZnO NPs. *Langmuir* **2011**, *27*, 4020–4028. [CrossRef]
40. Jiang, Y.; Zhang, L.; Wen, D.; Ding, Y. Role of physical and chemical interactions in the antibacterial behavior of ZnO NPs against *E. coli*. *Mater. Sci. Eng. C* **2016**, *69*, 1361–1366. [CrossRef]
41. Shi, L.E.; Fang, X.J.; Zhang, Z.L.; Zhou, T.; Jiang, D.; Wu, H.H.; Tang, Z.X. Preparation of nano-ZnO using sonication method and its antibacterial characteristics. *Int. J. Food Sci. Technol.* **2012**, *47*, 1866–1871. [CrossRef]
42. Nagarajan, P.; Vijayaraghavan, R. Enhanced bioactivity of ZnO NPs—An antimicrobial study. *Sci. Technol. Adv. Mater.* **2008**, *9*, 035004.
43. Ghule, K.; Ghule, A.V.; Chen, B.J.; Ling, Y.C. Preparation and characterization of ZnO NPs coated paper and its antibacterial activity study. *Green Chem.* **2006**, *8*, 1034–1041. [CrossRef]
44. Reddy, K.M.; Feris, K.; Bell, J.; Wingett, D.G.; Hanley, C.; Punnoose, A. Selective toxicity of ZnO NPs to prokaryotic and eukaryotic systems. *Appl. Phys. Lett.* **2007**, *90*, 213902. [CrossRef]
45. Sarwar, S.; Chakraborti, S.; Bera, S.; Sheikh, I.A.; Hoque, K.M.; Chakrabarti, P. The antimicrobial activity of ZnO NPs against *Vibrio cholerae*: Variation in response depends on biotype. *Nanomed. Nanotechnol. Biol. Med.* **2016**, *12*, 1499–1509. [CrossRef]
46. Soren, S.; Kumar, S.; Mishra, S.; Jena, P.K.; Verma, S.K.; Parhi, P. Evaluation of antibacterial and antioxidant potential of the ZnO NPs synthesized by aqueous and polyol method. *Microb. Pathog.* **2018**, *119*, 145–151. [CrossRef]
47. Babayevska, N.; Przysiecka, Ł.; Iatsunskyi, I.; Nowaczyk, G.; Jarek, M.; Janiszewska, E.; Jurga, S. ZnO size and shape effect on antibacterial activity and cytotoxicity profile. *Sci. Rep.* **2022**, *12*, 8148. [CrossRef]
48. Matai, I.; Sachdev, A.; Dubey, P.; Kumar, S.U.; Bhushan, B.; Gopinath, P. Antibacterial activity and mechanism of Ag–ZnO nanocomposite on *S. aureus* and GFP-expressing antibiotic resistant *E. coli*. *Colloids Surf. B Biointerfaces* **2014**, *115*, 359–367. [CrossRef]
49. Iswarya, A.; Vaseeharan, B.; Anjugam, M.; Ashokkumar, B.; Govindarajan, M.; Alharbi, N.S.; Kadaikunnan, S.; Khaled, J.M.; Benelli, G. Multipurpose efficacy of ZnO NPs coated by the crustacean immune molecule β-1, 3-glucan binding protein: Toxicity on HepG2 liver cancer cells and bacterial pathogens. *Colloids Surf. B Biointerfaces* **2017**, *158*, 257–269. [CrossRef]
50. Shaban, M.; Mohamed, F.; Abdallah, S. Production and characterization of superhydrophobic and antibacterial coated fabrics utilizing ZnO nanocatalyst. *Sci. Rep.* **2018**, *8*, 3925. [CrossRef]
51. Karthik, K.; Dhanuskodi, S.; Gobinath, C.; Sivaramakrishnan, S. Microwave-assisted synthesis of CdO–ZnO nanocomposite and its antibacterial activity against human pathogens. *Spectrochim. Acta Part A Mol. Biomol. Spectrosc.* **2015**, *139*, 7–12. [CrossRef]
52. Bellanger, X.; Billard, P.; Schneider, R.; Balan, L.; Merlin, C. Stability and toxicity of ZnO quantum dots: Interplay between NPs and bacteria. *J. Hazard. Mater.* **2015**, *283*, 110–116. [CrossRef]

53. Dědková, K.; Janíková., B.; Matějová, K.; Peikertová, P.; Neuwirthová, L.; Holešinský, J.; Kukutschová, J. Preparation, characterization and antibacterial properties of ZnO/kaoline nanocomposites. *J. Photochem. Photobiol. B Biol.* **2015**, *148*, 113–117. [CrossRef] [PubMed]
54. Ramani, M.; Ponnusamy, S.; Muthamizhchelvan, C.; Cullen, J.; Krishnamurthy, S.; Marsili, E. Morphology-directed synthesis of ZnO nanostructures and their antibacterial activity. *Colloids Surf. B Biointerfaces* **2013**, *105*, 24–30. [CrossRef] [PubMed]
55. Divya, M.; Vaseeharan, B.; Abinaya, M.; Vijayakumar, S.; Govindarajan, M.; Alharbi, N.S.; Kadaikunnan, S.; Khaled, J.M.; Benelli, G. Biopolymer gelatin-coated ZnO NPs showed high antibacterial, antibiofilm and anti-angiogenic activity. *J. Photochem. Photobiol. B Biol.* **2018**, *178*, 211–218. [CrossRef] [PubMed]
56. Wu, W.; Liu, T.; He, H.; Wu, X.; Cao, X.; Jin, J.; Sun, Q.; Roy, V.A.; Li, R.K. Rhelogical and antibacterial performance of sodium alginate/ZnO composite coating for cellulosic paper. *Colloids Surf. B Biointerfaces* **2018**, *167*, 538–543. [CrossRef] [PubMed]
57. Lee, J.; Choi, K.H.; Min, J.; Kim, H.J.; Jee, J.P.; Park, B.J. Functionalized ZnO NPs with gallic acid for antioxidant and antibacterial activity against methicillin-resistant *S. aureus*. *Nanomaterials* **2017**, *7*, 365. [CrossRef]
58. da Silva, B.L.; Abuçafy, M.P.; Manaia, E.B.; Junior, J.A.O.; Chiari-Andréo, B.G.; Pietro, R.C.R.; Chiavacci, L.A. Relationship between structure and antimicrobial activity of ZnO NPs: An overview. *Int. J. Nanomed.* **2019**, *14*, 9395. [CrossRef]
59. Dimkpa, C.O.; McLean, J.E.; Britt, D.W.; Anderson, A.J. Antifungal activity of ZnO NPs and their interactive effect with a biocontrol bacterium on growth antagonism of the plant pathogen *Fusarium graminearum*. *Biometals* **2013**, *26*, 913–924. [CrossRef]
60. Jamdagni, P.; Khatri, P.; Rana, J.S. Green synthesis of ZnO NPs using flower extract of *Nyctanthes arbortristis* and their antifungal activity. *J. King Saud Univ. Sci.* **2018**, *30*, 168–175. [CrossRef]
61. Arciniegas-Grijalba, P.A.; Patiño-Portela, M.C.; Mosquera-Sánchez, L.P.; Guerrero-Vargas, J.A.; Rodríguez-Páez, J.E. ZnO NPs (ZnO-NPs) and their antifungal activity against coffee fungus *Erythricium salmonicolor*. *Appl. Nanosci.* **2017**, *7*, 225–241. [CrossRef]
62. Erazo, A.; Mosquera, S.A.; Rodríguez-Paéz, J.E. Synthesis of ZnO NPs with different morphology: Study of their antifungal effect on strains of *Aspergillus niger* and *Botrytis cinerea*. *Mater. Chem. Phys.* **2019**, *234*, 172–184. [CrossRef]
63. He, L.; Liu, Y.; Mustapha, A.; Lin, M. Antifungal activity of ZnO NPs against *Botrytis cinerea* and *Penicillium expansum*. *Microbiol. Res.* **2011**, *166*, 207–215. [CrossRef]
64. Pariona, N.; Paraguay-Delgado, F.; Basurto-Cereceda, S.; Morales-Mendoza, J.E.; Hermida-Montero, L.A.; Mtz-Enriquez, A.I. Shape-dependent antifungal activity of ZnO particles against phytopathogenic fungi. *Appl. Nanosci.* **2020**, *10*, 435–443. [CrossRef]
65. Surendra, T.V.; Roopan, S.M.; Al-Dhabi, N.A.; Arasu, M.V.; Sarkar, G.; Suthindhiran, K. Vegetable Peel Waste for the Production of ZnO NPs and its Toxicological Efficiency, Antifungal, Hemolytic, and Antibacterial Activities. *Nanoscale Res. Lett.* **2016**, *11*, 546. [CrossRef]
66. Gunalan, S.; Sivaraj, R.; Rajendran, V. Green synthesized ZnO NPs against bacterial and fungal pathogens. *Prog. Nat. Sci. Mater. Int.* **2012**, *22*, 693–700. [CrossRef]
67. Jasim, N.O. Antifungal Activity of ZnO NPs on Aspergillus Fumigatus Fungus Candida Albicans Yeast. *Citeseer* **2015**, *5*, 23–28.
68. Decelis, S.; Sardella, D.; Triganza, T.; Brincat, J.-P.; Gatt, R.; Valdramidis, V.P. Assessing the anti-fungal efficiency of filters coated with ZnO NPs. *R. Soc. Open Sci.* **2017**, *4*, 1–9. [CrossRef]
69. Esteban-Tejeda, L.; Prado, C.; Cabal, B.; Sanz, J.; Torrecillas, R.; Moya, J.S. Antibacterial and antifungal activity of ZnO containing glasses. *PLoS ONE* **2015**, *10*, e0132709. [CrossRef]
70. Sierra-Fernandez, A.; De La Rosa-García, S.C.; Gomez-Villalba, L.S.; Gómez-Cornelio, S.; Rabanal, M.E.; Fort, R.; Quintana, P. Synthesis, Photocatalytic, and Antifungal Properties of MgO, ZnO and Zn/Mg Oxide NPs for the Protection of Calcareous Stone Heritage. *ACS Appl. Mater. Interfaces* **2017**, *9*, 24873–24886. [CrossRef]
71. Barad, S.; Roudbary, M.; Omran, N.A.; Daryasari, P.M. Preparation and characterization of ZnO NPs coated by chitosan-linoleic acid; fungal growth and biofilm assay. *Bratisl. Med. J. Bratisl. Lek. List.* **2017**, *118*, 169–174. [CrossRef]
72. Raman, C.D.; Kanmani, S. Textile dye degradation using nano zero valent iron: A review. *J. Environ. Manag.* **2016**, *177*, 341–355. [CrossRef]
73. Yulizar, Y.; Apriandanu, D.O.B.; Surya, R.M. Fabrication of novel SnWO4/ZnO using *Muntingia calabura* L. leaf extract with enhanced photocatalytic methylene blue degradation under visible light irradiation. *Ceram. Int.* **2022**, *48*, 3564–3577.
74. Ong, C.B.; Ng, L.Y.; Mohammad, A.W. A review of ZnO NPs as solar photocatalysts: Synthesis, mechanisms and applications. *Renew. Sustain. Energy Rev.* **2018**, *81*, 536–551. [CrossRef]
75. Wu, Y.; Altuner, E.E.; Tiri, R.N.E.H.; Bekmezci, M.; Gulbagca, F.; Aygun, A.; Xia, C.; Van Le, Q.; Sen, F.; Karimi-Maleh, H. Hydrogen generation from methanolysis of sodium borohydride using waste coffee oil modified ZnO NPs and their photocatalytic activities. *Int. J. Hydrog. Energy* **2022**, *in press*.
76. Davar, F.; Majedi, A.; Mirzaei, A. Green synthesis of ZnO NPs and its application in the degradation of some dyes. *J. Am. Ceram. Soc.* **2015**, *98*, 1739–1746. [CrossRef]
77. Rahman, Q.I.; Ahmad, M.; Misra, S.K.; Lohani, M. Effective photocatalytic degradation of rhodamine B dye by ZnO NPs. *Mater. Lett.* **2013**, *91*, 170–174. [CrossRef]
78. Hernández-Carrillo, M.A.; Torres-Ricárdez, R.; García-Mendoza, M.F.; Ramírez-Morales, E.; Rojas-Blanco, L.; Díaz-Flores, L.L.; Sepúlveda-Palacios, G.E.; Paraguay-Delgado, F.; Pérez-Hernández, G. Eu-modified ZnO NPs for applications in photocatalysis. *Catal. Today* **2020**, *349*, 191–197. [CrossRef]
79. Chen, M.; Liu, P.; He, J.H.; Wang, H.L.; Zhang, H.; Wang, X.; Chen, R. Nanofiber template-induced preparation of ZnO nanocrystal and its application in photocatalysis. *Sci. Rep.* **2021**, *11*, 1–8. [CrossRef]

80. Kumar, R.; Umar, A.; Kumar, G.; Akhtar, M.S.; Wang, Y.; Kim, S.H. Ce-doped ZnO NPs for efficient photocatalytic degradation of direct red-23 dye. *Ceram. Int.* **2015**, *41*, 7773–7782. [CrossRef]
81. Dar, G.N.; Umar, A.; Zaidi, S.A.; Ibrahim, A.A.; Abaker, M.; Baskoutas, S.; Al-Assiri, M.S. Ce-doped ZnO nanorods for the detection of hazardous chemical. *Sens. Actuators B Chem.* **2012**, *173*, 72–78. [CrossRef]
82. Buasakun, J.; Srilaoong, P.; Rattanakam, R.; Duangthongyou, T. Synthesis of Heterostructure of ZnO@MOF-46(Zn) to Improve the Photocatalytic Performance in Methylene Blue Degradation. *Crystals* **2021**, *11*, 1379. [CrossRef]
83. Gherab, K.; Al-Douri, Y.; Hashim, U.; Ameri, M.; Bouhemadou, A.; Batoo, K.M.; Adil, S.F.; Khan, M.; Raslan, E.H. Fabrication and characterizations of Al NPs doped ZnO nanostructures-based integrated electrochemical biosensor. *J. Mater. Res. Technol.* **2020**, *9*, 857–867. [CrossRef]
84. Tu, W.; Lei, J.; Wang, P.; Ju, H. Photoelectrochemistry of Free-Base-Porphyrin-Functionalized ZnO NPs and Their Applications in Biosensing. *Chem. A Eur. J.* **2011**, *17*, 9440–9447. [CrossRef]
85. Inbasekaran, S.; Senthil, R.; Ramamurthy, G.; Sastry, T.P. Biosensor using ZnO NPs. *Int. J. Innov. Res. Sci. Eng. Technol.* **2014**, *3*, 8601–8606.
86. Napi, M.L.M.; Sultan, S.M.; Ismail, R.; How, K.W.; Ahmad, M.K. Electrochemical-based biosensors on different ZnO nanostructures: A review. *Materials* **2019**, *12*, 2985. [CrossRef]
87. Arya, S.K.; Saha, S.; Ramirez-Vick, J.E.; Gupta, V.; Bhansali, S.; Singh, S.P. Recent advances in ZnO nanostructures and thin films for biosensor applications. *Anal. Chim. Acta* **2012**, *737*, 1–21. [CrossRef]
88. Wang, G.; Tan, X.; Zhou, Q.; Liu, Y.; Wang, M.; Yang, L. Synthesis of highly dispersed ZnO NPs on carboxylic graphene for development a sensitive acetylcholinesterase biosensor. *Sens. Actuators B Chem.* **2014**, *190*, 730–736. [CrossRef]
89. Kim, H.M.; Park, J.H.; Lee, S.K. Fiber optic sensor based on ZnO nanowires decorated by Au nanoparticles for improved plasmonic biosensor. *Sci. Rep.* **2019**, *9*, 15605. [CrossRef]
90. Devi, R.; Yadav, S.; Pundir, C.S. Amperometric determination of xanthine in fish meat by ZnO nanoparticle/chitosan/multiwalled carbon nanotube/polyaniline composite film bound xanthine oxidase. *Analyst* **2012**, *137*, 754–759. [CrossRef]
91. Siddiquee, S.; Yusof, N.A.; Salleh, A.B.; Tan, S.G.; Bakar, F.A. Development of electrochemical DNA biosensor for Trichoderma harzianum based on ionic liquid/ZnO NPs/chitosan/gold electrode. *J. Solid State Electrochem.* **2012**, *16*, 273–282. [CrossRef]
92. Haghighi, B.; Bozorgzadeh, S. Fabrication of a highly sensitive electrochemiluminescence lactate biosensor using ZnO NPs decorated multiwalled carbon nanotubes. *Talanta* **2011**, *85*, 2189–2193. [CrossRef]
93. Supraja, P.; Singh, V.; Vanjari, S.R.K.; Govind Singh, S. Electrospun CNT embedded ZnO nanofiber based biosensor for electrochemical detection of Atrazine: A step closure to single molecule detection. *Microsyst. Nanoeng.* **2020**, *6*, 3. [CrossRef] [PubMed]
94. Umar, A.; Rahman, M.M.; Vaseem, M.; Hahn, Y.B. Ultra-sensitive cholesterol biosensor based on low-temperature grown ZnO NPs. *Electrochem. Commun.* **2009**, *11*, 118–121. [CrossRef]
95. Khan, R.; Kaushik, A.; Solanki, P.R.; Ansari, A.A.; Pandey, M.K.; Malhotra, B.D. ZnO NPs-chitosan composite film for cholesterol biosensor. *Anal. Chim. Acta* **2008**, *616*, 207–213. [CrossRef] [PubMed]
96. Vasudevan, S.; Srinivasan, P.; Rayappan, J.B.B.; Solomon, A.P. A photoluminescence biosensor for the detection of N-acyl homoserine lactone using cysteamine functionalized ZnO NPs for the early diagnosis of urinary tract infections. *J. Mater. Chem. B* **2020**, *8*, 4228–4236. [CrossRef]
97. Wang, Y.; Yu, L.; Zhu, Z.; Zhang, J.; Zhu, J. Novel uric acid sensor based on enzyme electrode modified by zno NPs and multiwall carbon nanotubes. *Anal. Lett.* **2009**, *42*, 775–789. [CrossRef]
98. Sadeghi, R.; Karimi-Maleh, H.; Bahari, A.; Taghavi, M. A novel biosensor based on ZnO nanoparticle/1, 3-dipropylimidazolium bromide ionic liquid-modified carbon paste electrode for square-wave voltammetric determination of epinephrine. *Phys. Chem. Liq.* **2013**, *51*, 704–714. [CrossRef]
99. Ali, A.; Ansari, A.A.; Kaushik, A.; Solanki, P.R.; Barik, A.; Pandey, M.K.; Malhotra, B.D. Nanostructured ZnO film for urea sensor. *Mater. Lett.* **2009**, *63*, 2473–2475. [CrossRef]
100. Aydoğdu, G.; Zeybek, D.K.; Pekyardımcı, Ş.; Kılıç, E. A novel amperometric biosensor based on ZnO NPs-modified carbon paste electrode for determination of glucose in human serum. *Artif. Cells Nanomed. Biotechnol.* **2013**, *41*, 332–338. [CrossRef]
101. Aini, B.N.; Siddiquee, S.; Ampon, K.; Rodrigues, K.F.; Suryani, S. Development of glucose biosensor based on ZnO NPs film and glucose oxidase-immobilized eggshell membrane. *Sens. Bio-Sens. Res.* **2015**, *4*, 46–56. [CrossRef]
102. Shukla, S.K.; Deshpande, S.R.; Shukla, S.K.; Tiwari, A. Fabrication of a tunable glucose biosensor based on ZnO/chitosan-graft-poly (vinyl alcohol) core-shell nanocomposite. *Talanta* **2012**, *99*, 283–287. [CrossRef]
103. Chawla, S.; Pundir, C.S. An amperometric hemoglobin A1c biosensor based on immobilization of fructosyl amino acid oxidase onto ZnO NPs–polypyrrole film. *Anal. Biochem.* **2012**, *430*, 156–162. [CrossRef]
104. Huang, Q.; Wang, Y.; Lei, L.; Xu, Z.; Zhang, W. Photoelectrochemical biosensor for acetylcholinesterase activity study based on metal oxide semiconductor nanocomposites. *J. Electroanal. Chem.* **2016**, *781*, 377–382. [CrossRef]
105. Wang, Y.T.; Bao, Y.J.; Lou, L.; Li, J.J.; Du, W.J.; Zhu, Z.Q.; Peng, H.; Zhu, J.Z. A novel L-lactate sensor based on enzyme electrode modified with ZnO NPs and multiwall carbon nanotubes. In *SENSORS, 2010 IEEE, Waikoloa, HI, USA, 1–4 November 2010*; IEEE: Piscataway, NJ, USA, 2010; pp. 33–37.
106. Li, X.; Zhao, C.; Liu, X. A paper-based microfluidic biosensor integrating ZnO nanowires for electrochemical glucose detection. *Microsyst. Nanoeng.* **2015**, *1*, 15014. [CrossRef]

107. Danielson, E.; Dhamodharan, V.; Porkovich, A.; Kumar, P.; Jian, N.; Ziadi, Z.; Grammatikopoulos, P.; Sontakke, V.A.; Yokobayashi, Y.; Sowwan, M. Gas-phase ynthesis for label-free biosensors: Zinc-oxide nanowires functionalized with gold NPs. *Sci. Rep.* **2019**, *9*, 17370. [CrossRef]
108. Rong, P.; Ren, S.; Yu, Q. Fabrications and applications of ZnO NMs in flexible functional devices—A review. *Crit. Rev. Anal. Chem.* **2019**, *49*, 336–349. [CrossRef]
109. Salinas, R.A.; Orduña-Díaz, A.; Obregon-Hinostroza, O.; Dominguez, M.A. Biosensors based on ZnO thin-film transistors using recyclable plastic substrates as an alternative for real-time pathogen detection. *Talanta* **2022**, *237*, 122970. [CrossRef]
110. Mansoor, S.; Shahid, S.; Ashiq, K.; Alwadai, N.; Javed, M.; Iqbal, S.; Fatima, U.; Zaman, S.; Sarwar, M.N.; Alshammari, F.H.; et al. Controlled growth of nanocomposite thin layer based on Zn-Doped MgO NPs through Sol-Gel technique for biosensor applications. *Inorg. Chem. Commun.* **2022**, *142*, 109702. [CrossRef]
111. Zhang, X.; Villafuerte, J.; Consonni, V.; Sarigiannidou, E.; Capsal, J.F.; Bruhat, A.; Grinberg, D.; Petit, L.; Cottinet, P.J.; Le, M.Q. Optimization Strategies Used for Boosting Piezoelectric Response of Biosensor Based on Flexible Micro-ZnO Composites. *Biosensors* **2022**, *12*, 245. [CrossRef]
112. Mahmoud, A.; Echabaane, M.; Omri, K.; Boudon, J.; Saviot, L.; Millot, N.; Chaabane, R.B. Cu-Doped ZnO NPs for Non-Enzymatic Glucose Sensing. *Molecules* **2021**, *26*, 929. [CrossRef]
113. Vijayaprasath, G.; Murugan, R.; Narayanan, J.S.; Dharuman, V.; Ravi, G.; Hayakawa, Y. Glucose sensing behavior of cobalt doped ZnO NPs synthesized by co-precipitation method. *J. Mater. Sci. Mater. Electron.* **2015**, *26*, 4988–4996. [CrossRef]
114. Raza, W.; Ahmad, K. A highly selective Fe@ ZnO modified disposable screen printed electrode based non-enzymatic glucose sensor (SPE/Fe@ ZnO). *Mater. Lett.* **2018**, *212*, 231–234. [CrossRef]
115. Guan, H.N.; Chi, D.F.; Yu, J. Photoelectrochemical acetylcholinesterase biosensor incorporating ZnO NPs. In *Advanced Materials Research*; Trans Tech Publications Ltd.: Wollerau, Switzerland, 2011; Volume 183, pp. 1701–1706.
116. Singh, S.P.; Arya, S.K.; Pandey, P.; Malhotra, B.D.; Saha, S.; Sreenivas, K.; Gupta, V. Cholesterol biosensor based on rf sputtered ZnO nanoporous thin film. *Appl. Phys. Lett.* **2007**, *91*, 063901. [CrossRef]
117. Solanki, P.R.; Kaushik, A.; Ansari, A.A.; Malhotra, B.D. Nanostructured ZnO platform for cholesterol sensor. *Appl. Phys. Lett.* **2009**, *94*, 143901. [CrossRef]
118. Zhao, Y.; Fang, X.; Gu, Y.; Yan, X.; Kang, Z.; Zheng, X.; Lin, P.; Zhao, L.; Zhang, Y. Gold NPs coated ZnO nanorods as the matrix for enhanced l-lactate sensing. *Colloids Surf. B Biointerfaces* **2015**, *126*, 476–480. [CrossRef] [PubMed]
119. Subhan, M.A.; Saha, P.C.; Hossain, A.; Asiri, A.M.; Alam, M.M.; Al-Mamun, M.; Ghann, W.; Uddin, J.; Raihan, T.; Azad, A.K.; et al. Photocatalytic performance, anti-bacterial activities and 3-chlorophenol sensor fabrication using $MnAl_2O_4 \cdot ZnAl_2O_4$ NMs. *Nanoscale Adv.* **2021**, *3*, 5872–5889. [CrossRef]
120. Sruthi, S.; Ashtami, J.; Mohanan, P.V. Biomedical application and hidden toxicity of ZnO NPs. *Mater. Today Chem.* **2018**, *10*, 175–186. [CrossRef]
121. Senthilkumar, K.; Senthilkumar, O.; Yamauchi, K.; Sato, M.; Morito, S.; Ohba, T.; Nakamura, M.; Fujita, Y. Preparation of ZnO NPs for bio-imaging applications. *Phys. Status Solidi* **2009**, *246*, 885–888. [CrossRef]
122. Wu, Y.L.; Lim, C.S.; Fu, S.; Tok, A.I.Y.; Lau, H.M.; Boey, F.Y.C.; Zeng, X.T. Surface modifications of ZnO quantum dots for bio-imaging. *Nanotechnology* **2007**, *18*, 215604. [CrossRef]
123. Liu, Y.; Ai, K.; Yuan, Q.; Lu, L. Fluorescence-enhanced gadolinium-doped ZnO quantum dots for magnetic resonance and fluorescence imaging. *Biomaterials* **2011**, *32*, 1185–1192. [CrossRef]
124. Gupta, J.; Hassan, P.A.; Barick, K.C. Core-shell Fe3O4@ ZnO NPs for magnetic hyperthermia and bio-imaging applications. *AIP Adv.* **2021**, *11*, 025207. [CrossRef]
125. Kumawat, A.; Chattopadhyay, S.; Verma, R.K.; Misra, K.P. Eu doped ZnO NPs with strong potential of thermal sensing and bioimaging. *Mater. Lett.* **2022**, *308*, 131221. [CrossRef]
126. Dey, A.; Ray, P.G.; Dhara, S.; Neogi, S. Optically engineered ZnO NPs: Excitable at visible wavelength and lowered cytotoxicity towards bioimaging applications. *Appl. Surf. Sci.* **2022**, *592*, 153303. [CrossRef]
127. Abadjian, M.C.Z.; Choi, J.; Anderson, C.J. NPs for PET imaging of tumors and cancer metastasis. In *Design and Applications of NPs in Biomedical Imaging*; Springer: Cham, Switzerland, 2017; pp. 229–255.
128. Li, Y.; Wang, R.; Zheng, W.; Li, Y. Silica-Coated Ga (III)-Doped ZnO: $Yb^{3+}$, $Tm^{3+}$ Upconversion NPs for High-Resolution in Vivo Bioimaging using Near-Infrared to Near-Infrared Upconversion Emission. *Inorg. Chem.* **2019**, *58*, 8230–8236. [CrossRef]
129. Eriksson, J.; Khranovskyy, V.; Söderlind, F.; Käll, P.O.; Yakimova, R.; Spetz, A.L. ZnO NPs or ZnO films: A comparison of the gas sensing capabilities. *Sens. Actuators B Chem.* **2009**, *137*, 94–102. [CrossRef]
130. Fan, F.; Feng, Y.; Bai, S.; Feng, J.; Chen, A.; Li, D. Synthesis and gas sensing properties to $NO_2$ of ZnO NPs. *Sens. Actuators B Chem.* **2013**, *185*, 377–382. [CrossRef]
131. Bian, H.; Ma, S.; Sun, A.; Xu, X.; Yang, G.; Yan, S.; Gao, J.; Zhang, Z.; Zhu, H. Improvement of acetone gas sensing performance of ZnO NPs. *J. Alloys Compd.* **2016**, *658*, 629–635. [CrossRef]
132. Tang, H.; Yan, M.; Ma, X.; Zhang, H.; Wang, M.; Yang, D. Gas sensing behavior of polyvinylpyrrolidone-modified ZnO NPs for trimethylamine. *Sens. Actuators B Chem.* **2006**, *113*, 324–328. [CrossRef]
133. Umar, A.; Khan, M.A.; Kumar, R.; Algarni, H. Ag-doped ZnO NPs for enhanced ethanol gas sensing application. *J. Nanosci. Nanotechnol.* **2018**, *18*, 3557–3562. [CrossRef]

134. Yan, H.; Song, P.; Zhang, S.; Yang, Z.; Wang, Q. Facile synthesis, characterization and gas sensing performance of ZnO NPs-coated $MoS_2$ nanosheets. *J. Alloys Compd.* **2016**, *662*, 118–125. [CrossRef]
135. Zhang, D.; Yang, Z.; Li, P.; Zhou, X. Ozone gas sensing properties of metal-organic frameworks-derived $In_2O_3$ hollow microtubes decorated with ZnO NPs. *Sens. Actuators B Chem.* **2019**, *301*, 127081. [CrossRef]
136. Jagannathan, M.; Dhinasekaran, D.; Rajendran, A.R.; Subramaniam, B. Selective room temperature ammonia gas sensor using nanostructured ZnO/CuO@ graphene on paper substrate. *Sens. Actuators B Chem.* **2022**, *350*, 130833. [CrossRef]
137. Franco, M.A.; Conti, P.P.; Andre, R.S.; Correa, D.S. A review on chemiresistive ZnO gas sensors. *Sens. Actuators Rep.* **2022**, *4*, 100100. [CrossRef]
138. Ancona, A.; Dumontel, B.; Garino, N.; Demarco, B.; Chatzitheodoridou, D.; Fazzini, W.; Engelke, H.; Cauda, V. Lipid-coated ZnO NPs as innovative ROS-generators for photodynamic therapy in cancer cells. *Nanomaterials* **2018**, *8*, 143. [CrossRef] [PubMed]
139. Sudhagar, S.; Sathya, S.; Pandian, K.; Lakshmi, B.S. Targeting and sensing cancer cells with ZnO nanoprobes in vitro. *Biotechnol. Lett.* **2011**, *33*, 1891–1896. [CrossRef] [PubMed]
140. Bisht, G.; Rayamajhi, S. ZnO NPs: A promising anticancer agent. *Nanobiomedicine* **2016**, *3*, 3–9. [CrossRef]
141. Sathishkumar, P.; Li, Z.; Govindan, R.; Jayakumar, R.; Wang, C.; Gu, F.L. ZnO-quercetin nanocomposite as a smart nano-drug delivery system: Molecular-level interaction studies. *Appl. Surf. Sci.* **2021**, *536*, 147741. [CrossRef]
142. Peng, H.; Cui, B.; Li, G.; Wang, Y.; Li, N.; Chang, Z.; Wang, Y. A multifunctional β-CD-modified $Fe_3O_4$@ ZnO: $Er^{3+}$, $Yb^{3+}$ nanocarrier for antitumor drug delivery and microwave-triggered drug release. *Mater. Sci. Eng. C* **2015**, *46*, 253–263. [CrossRef]
143. Tan, L.; Liu, J.; Zhou, W.; Wei, J.; Peng, Z. A novel thermal and pH responsive drug delivery system based on ZnO@ PNIPAM hybrid NPs. *Mater. Sci. Eng. C* **2014**, *45*, 524–529. [CrossRef]
144. Zhao, Q.G.; Wang, J.; Zhang, Y.P.; Zhang, J.; Tang, A.N.; Kong, D.M. A ZnO-gated porphyrinic metal–organic framework-based drug delivery system for targeted bimodal cancer therapy. *J. Mater. Chem. B* **2018**, *6*, 7898–7907. [CrossRef]
145. Vijayakumar, S.; Saravanakumar, K.; Malaikozhundan, B.; Divya, M.; Vaseeharan, B.; Durán-Lara, E.F.; Wang, M.H. Biopolymer K-carrageenan wrapped ZnO NPs as drug delivery vehicles for anti MRSA therapy. *Int. J. Biol. Macromol.* **2020**, *144*, 9–18. [CrossRef]
146. Chen, T.; Zhao, T.; Wei, D.; Wei, Y.; Li, Y.; Zhang, H. Core–shell nanocarriers with ZnO quantum dots-conjugated Au nanoparticle for tumor-targeted drug delivery. *Carbohydr. Polym.* **2013**, *92*, 1124–1132. [CrossRef]
147. Afzal, H.; Ikram, M.; Ali, S.; Shahzadi, A.; Aqeel, M.; Haider, A.; Imran, M. Enhanced drug efficiency of doped ZnO–GO (graphene oxide) nanocomposites, a new gateway in drug delivery systems (DDSs). *Mater. Res. Express* **2020**, *7*, 015405. [CrossRef]
148. Yadollahi, M.; Farhoudian, S.; Barkhordari, S.; Gholamali, I.; Farhadnejad, H.; Motasadizadeh, H. Facile synthesis of chitosan/ZnO bio-nanocomposite hydrogel beads as drug delivery systems. *Int. J. Biol. Macromol.* **2016**, *82*, 273–278. [CrossRef]
149. Yuan, Q.; Hein, S.; Misra, R.D.K. New generation of chitosan-encapsulated ZnO quantum dots loaded with drug: Synthesis, characterization and in vitro drug delivery response. *Acta Biomater.* **2010**, *6*, 2732–2739. [CrossRef]
150. Qiu, H.; Cui, B.; Li, G.; Yang, J.; Peng, H.; Wang, Y.; Li, N.; Gao, R.; Chang, Z.; Wang, Y. Novel $Fe_3O_4$@ ZnO@ $mSiO_2$ nanocarrier for targeted drug delivery and controllable release with microwave irradiation. *J. Phys. Chem. C* **2014**, *118*, 14929–14937. [CrossRef]
151. Wu, S.; Huang, X.; Du, X. pH-and redox-triggered synergistic controlled release of a ZnO-gated hollow mesoporous silica drug delivery system. *J. Mater. Chem. B* **2015**, *3*, 1426–1432. [CrossRef]
152. Cai, X.; Luo, Y.; Zhang, W.; Du, D.; Lin, Y. pH-Sensitive ZnO quantum dots–doxorubicin NPs for lung cancer targeted drug delivery. *ACS Appl. Mater. Interfaces* **2016**, *8*, 22442–22450. [CrossRef]
153. Xiong, H.M. ZnO NPs applied to bioimaging and drug delivery. *Adv. Mater.* **2013**, *25*, 5329–5335. [CrossRef]
154. Zheng, C.; Wang, Y.; Phua, S.Z.F.; Lim, W.Q.; Zhao, Y. ZnO–DOX@ ZIF-8 core–shell NPs for pH-responsive drug delivery. *ACS Biomater. Sci. Eng.* **2017**, *3*, 2223–2229. [CrossRef]
155. Martínez-Carmona, M.; Gun'Ko, Y.; Vallet-Regí, M. ZnO nanostructures for drug delivery and theranostic applications. *Nanomaterials* **2018**, *8*, 268. [CrossRef]
156. Wang, J.; Lee, J.S.; Kim, D.; Zhu, L. Exploration of Zinc Oxide Nanoparticles as a Multitarget and Multifunctional Anticancer Nanomedicine. *ACS Appl. Mater. Interfaces* **2017**, *9*, 39971–39984. [CrossRef] [PubMed]
157. Vimala, K.; Shanthi, K.; Sundarraj, S.; Kannan, S. Synergistic effect of chemo-photothermal for breast cancer therapy using folic acid (FA) modified zinc oxide nanosheet. *J. Colloid Interface Sci.* **2017**, *488*, 92–108. [CrossRef] [PubMed]
158. Handford, C.E.; Dean, M.; Henchion, M.; Spence, M.; Elliott, C.T.; Campbell, K. Implications of nanotechnology for the agri-food industry: Opportunities, benefits and risks. *Trends Food Sci. Technol.* **2014**, *40*, 226–241. [CrossRef]
159. He, X.; Hwang, H.M. Nanotechnology in food science: Functionality, applicability, and safety assessment. *J. Food Drug Anal.* **2016**, *24*, 671–681. [CrossRef] [PubMed]
160. Das, S.; Sinha, S.; Das, B.; Jayabalan, R.; Suar, M.; Mishra, A.; Tamhankar, A.J.; Stålsby Lundborg, C.; Tripathy, S.K. Disinfection of multidrug resistant Escherichia coli by solar-photocatalysis using Fe-doped ZnO nanoparticles. *Sci. Rep.* **2017**, *7*, 104. [CrossRef] [PubMed]
161. Nesakumar, N.; Thandavan, K.; Sethuraman, S.; Krishnan, U.M.; Rayappan, J.B.B. nanorods an electrochemical biosensor with nanointerface for lactate detection based on lactate dehydrogenase immobilized on ZnO. *J. Colloid Interface Sci.* **2014**, *414*, 90–96. [CrossRef]
162. Zhao, Y.; Yan, X.; Kang, Z.; Fang, X.; Zheng, X.; Zhao, L.; Du, H.; Zhang, Y. ZnO nanowires-based electrochemical biosensor for L-lactic acid amperometric detection. *J. Nanoparticle Res.* **2014**, *16*, 1–9. [CrossRef]

163. Tayel, A.A.; El-Tras, W.F.; Moussa, S.; El-Baz, A.F.; Mahrous, H.; Salem, M.F.; Brimer, L. Antibacterial action of ZnO NPs against foodborne pathogens. *J. Food Saf.* **2011**, *31*, 211–218. [CrossRef]
164. Yadav, S.; Mehrotra, G.K.; Dutta, P.K. Chitosan based ZnO NPs loaded gallic-acid films for active food packaging. *Food Chem.* **2021**, *334*, 127605. [CrossRef]
165. Kumar, S.; Thakur, A.; Rangra, V.S.; Sharma, S. Synthesis and use of low-band-gap ZnO NPs for water treatment. *Arab. J. Sci. Eng.* **2016**, *41*, 2393–2398. [CrossRef]
166. Tankhiwale, R.; Bajpai, S.K. Preparation, characterization and antibacterial applications of ZnO-NPs coated polyethylene films for food packaging. *Colloids Surf. B Biointerfaces* **2012**, *90*, 16–20. [CrossRef]
167. Emerald, F.M.E.; Pushpadass, H.A.; Joseph, D.; Jaya, S.V. *Impact of Nanotechnology in Beverage Processing*; Elsevier: Amsterdam, The Netherlands, 2021.
168. Khalafi, T.; Buazar, F.; Ghanemi, K. Phycosynthesis and enhanced photocatalytic activity of ZnO NPs toward organosulfur pollutants. *Sci. Rep.* **2019**, *9*, 6866. [CrossRef]
169. Rameshbabu, R.; Kumar, N.; Karthigeyan, A.; Neppolian, B. Visible light photocatalytic activities of ZnFe2O4/ZnO NPs for the degradation of organic pollutants. *Mater. Chem. Phys.* **2016**, *181*, 106–115. [CrossRef]
170. Li, J.; Liu, L.; Liang, Q.; Zhou, M.; Yao, C.; Xu, S.; Li, Z. Core-shell ZIF-8@ MIL-68 (In) derived ZnO NPs-embedded $In_2O_3$ hollow tubular with oxygen vacancy for photocatalytic degradation of antibiotic pollutant. *J. Hazard. Mater.* **2021**, *414*, 125395. [CrossRef]
171. Pathakoti, K.; Manubolu, M.; Hwang, H.M. Nanotechnology applications for environmental industry. In *Handbook of NMs for Industrial Applications*; Elsevier: Amsterdam, The Netherlands, 2018; pp. 894–907.
172. Saravanan, R.; Gracia, F.; Khan, M.M.; Poornima, V.; Gupta, V.K.; Narayanan, V.; Stephen, A. ZnO/CdO nanocomposites for textile effluent degradation and electrochemical detection. *J. Mol. Liq.* **2015**, *209*, 374–380. [CrossRef]
173. Saravanan, R.; Karthikeyan, N.; Gupta, V.K.; Thirumal, E.; Thangadurai, P.; Narayanan, V.; Stephen, A. ZnO/Ag nanocomposite: An efficient catalyst for degradation studies of textile effluents under visible light. *Mater. Sci. Eng. C* **2013**, *33*, 2235–2244. [CrossRef] [PubMed]
174. Sathishkumar, P.; Sweena, R.; Wu, J.J.; Anandan, S. Synthesis of CuO-ZnO nanophotocatalyst for visible light assisted degradation of a textile dye in aqueous solution. *Chem. Eng. J.* **2011**, *171*, 136–140. [CrossRef]
175. Xie, H.; Ye, X.; Duan, K.; Xue, M.; Du, Y.; Ye, W.; Wang, C. CuAu–ZnO–graphene nanocomposite: A novel graphene-based bimetallic alloy-semiconductor catalyst with its enhanced photocatalytic degradation performance. *J. Alloys Compd.* **2015**, *636*, 40–47. [CrossRef]
176. Danwittayakul, S.; Jaisai, M.; Dutta, J. Efficient solar photocatalytic degradation of textile wastewater using ZnO/ZTO composites. *Appl. Catal. B Environ.* **2015**, *163*, 1–8. [CrossRef]
177. Qian, C.; Yin, J.; Zhao, J.; Li, X.; Wang, S.; Bai, Z.; Jiao, T. Facile preparation and highly efficient photodegradation performances of self-assembled Artemia eggshell-ZnO nanocomposites for wastewater treatment. *Colloids Surf. A Physicochem. Eng. Asp.* **2021**, *610*, 125752. [CrossRef]
178. Campagnolo, L.; Lauciello, S.; Athanassiou, A.; Fragouli, D. Au/ZnO hybrid nanostructures on electrospun polymeric mats for improved photocatalytic degradation of organic pollutants. *Water* **2019**, *11*, 1787. [CrossRef]
179. Akkari, M.; Aranda, P.; Mayoral, A.; García-Hernández, M.; Amara, A.B.H.; Ruiz-Hitzky, E. Sepiolite nanoplatform for the simultaneous assembly of magnetite and ZnO NPs as photocatalyst for improving removal of organic pollutants. *J. Hazard. Mater.* **2017**, *340*, 281–290. [CrossRef] [PubMed]
180. Elmi, F.; Alinezhad, H.; Moulana, Z.; Salehian, F.; Mohseni Tavakkoli, S.; Asgharpour, F.; Fallah, H.; Elmi, M.M. The use of antibacterial activity of ZnO NPs in the treatment of municipal wastewater. *Water Sci. Technol.* **2014**, *70*, 763–770. [CrossRef] [PubMed]
181. Asif, A.K.M.A.H.; Hasan, M.Z. Application of nanotechnology in modern textiles: A review. *Int. J. Curr. Eng. Technol.* **2018**, *8*, 227–231.
182. Yetisen, A.K.; Qu, H.; Manbachi, A.; Butt, H.; Dokmeci, M.R.; Hinestroza, J.P.; Skorobogatiy, M.; Khademhosseini, A.; Yun, S.H. Nanotechnology in textiles. *ACS Nano* **2016**, *10*, 3042–3068. [CrossRef]
183. Dimapilis, E.A.S.; Hsu, C.S.; Mendoza, R.M.O.; Lu, M.C. Zinc oxide nanoparticles for water disinfection. *Sustain. Environ. Res.* **2018**, *28*, 47–56. [CrossRef]
184. Raj, S.; Jose, S.; Sumod, U.S.; Sabitha, M. Nanotechnology in cosmetics: Opportunities and challenges. *J. Pharm. Bioallied Sci.* **2012**, *4*, 186. [CrossRef]
185. Katz, L.M.; Dewan, K.; Bronaugh, R.L. Nanotechnology in cosmetics. *Food Chem. Toxicol.* **2015**, *85*, 127–137. [CrossRef]
186. Garcia-Mesa, J.C.; Montoro-Leal, P.; Rodriguez-Moreno, A.; Guerrero, M.L.; Alonso, E.V. Direct solid sampling for speciation of $Zn^{2+}$ and ZnO NPs in cosmetics by graphite furnace atomic absorption spectrometry. *Talanta* **2021**, *223*, 121795. [CrossRef]
187. Osmond, M.J.; Mccall, M.J. ZnO NPs in modern sunscreens: An analysis of potential exposure and hazard. *Nanotoxicology* **2010**, *4*, 15–41. [CrossRef]
188. Lu, P.J.; Huang, S.C.; Chen, Y.P.; Chiueh, L.C.; Shih, D.Y.C. Analysis of titanium dioxide and ZnO NPs in cosmetics. *J. Food Drug Anal.* **2015**, *23*, 587–594. [CrossRef] [PubMed]
189. Adebayo-Tayo, B.C.; Borode, S.O.; Olaniyi, O.A. Phytosynthesis of ZnO NPs using methanol extract of *Senna alata* leaf: Characterization, optimization, antimicrobial properties, and its application in cold cream formulation. *Polym. Med.* **2020**, *50*, 5–19. [CrossRef]

190. Sonia, S.; Ruckmani, K.; Sivakumar, M. Antimicrobial and antioxidant potentials of biosynthesized colloidal ZnO NPs for a fortified cold cream formulation: A potent nanocosmeceutical application. *Mater. Sci. Eng. C* **2017**, *79*, 581–589.
191. Dkhil, M.A.; Diab, M.S.; Aljawdah, H.M.; Murshed, M.; Hafiz, T.A.; Al-Quraishy, S.; Bauomy, A.A. Neuro-biochemical changes induced by ZnO NPs. *Saudi J. Biol. Sci.* **2020**, *27*, 2863–2867. [CrossRef] [PubMed]
192. Norouzzadeh Helali, Z.; Esmailzadeh, M. A comparative study of antibacterial effects of mouthwashes containing Ag/ZnO or ZnO NPs with chlorhexidine and investigation of their cytotoxicity. *Nanomed. J.* **2018**, *5*, 102–110.
193. Soleimani, H.; Baig, M.K.; Yahya, N.; Khodapanah, L.; Sabet, M.; Demiral, B.M.; Burda, M. Synthesis of ZnO NPs for oil–water interfacial tension reduction in enhanced oil recovery. *Appl. Phys. A* **2018**, *124*, 1–13. [CrossRef]
194. Sayyadnejad, M.A.; Ghaffarian, H.R.; Saeidi, M. Removal of hydrogen sulfide by ZnO NPs in drilling fluid. *Int. J. Environ. Sci. Technol.* **2008**, *5*, 565–569. [CrossRef]
195. Alnarabiji, M.S.; Yahya, N.; Bee Abd Hamid, S.; Azizli, K.A.; Shafie, A.; Solemani, H. Microwave synthesis of ZnO NPs for enhanced oil recovery. In *Advanced Materials Research*; Trans Tech Publications Ltd.: Wollerau, Switzerland, 2014; Volume 1024, pp. 83–86.
196. Najafi, V.; Zolghadr, S.; Kimiagar, S. Remarkable reproducibility and significant sensitivity of ZnO NPs covered by Chromium (III) oxide as a hydrogen sulfide gas sensor. *Optik* **2019**, *182*, 249–256. [CrossRef]
197. Zhu, B.L.; Zeng, D.W.; Wu, J.; Song, W.L.; Xie, C.S. Synthesis and gas sensitivity of In-doped ZnO NPs. *J. Mater. Sci. Mater. Electron.* **2003**, *14*, 521–526. [CrossRef]
198. Liu, S.; Yu, B.; Zhang, H.; Fei, T.; Zhang, T. Enhancing $NO_2$ gas sensing performances at room temperature based on reduced graphene oxide-ZnO NPs hybrids. *Sens. Actuators B Chem.* **2014**, *202*, 272–278. [CrossRef]
199. Zhu, B.L.; Xie, C.S.; Zeng, D.W.; Song, W.L.; Wang, A.H. Investigation of gas sensitivity of Sb-doped ZnO NPs. *Mater. Chem. Phys.* **2005**, *89*, 148–153. [CrossRef]
200. Tajmiri, M.; Ehsani, M.R. The potential of ZnO NPs to reduce water consuming in iranian heavy oil reservoir. *J. Water Environ. Nanotechnol.* **2016**, *1*, 84–90.
201. Tajmiri, M.; Ehsani, M.R.; Mousavi, S.M.; Roayaei, E.; Emadi, A. The effect of ZnO NPs on improved oil recovery in spontaneous imbibition mechanism of heavy oil production. In *AIP Conference Proceedings*; AIP Publishing LLC.: Melville, NY, USA, 2015; Volume 1669, p. 020024.
202. Ismail, W.; Alhamad, N.A.; El-Sayed, W.S.; El Nayal, A.M.; Chiang, Y.R.; Hamzah, R.Y. Bacterial degradation of the saturate fraction of Arabian light crude oil: Biosurfactant production and the effect of ZnO NPs. *J. Pet. Environ. Biotechnol.* **2013**, *4*, 163.
203. Zheng, Z.Q.; Yao, J.D.; Wang, B.; Yang, G.W. Light-controlling, flexible and transparent ethanol gas sensor based on ZnO NPs for wearable devices. *Sci. Rep.* **2015**, *5*, 1–8.
204. Morgenstern, F.S.; Kabra, D.; Massip, S.; Brenner, T.J.; Lyons, P.E.; Coleman, J.N.; Friend, R.H. Ag-nanowire films coated with ZnO NPs as a transparent electrode for solar cells. *Appl. Phys. Lett.* **2011**, *99*, 242. [CrossRef]
205. Suliman, A.E.; Tang, Y.; Xu, L. Preparation of ZnO NPs and nanosheets and their application to dye-sensitized solar cells. *Sol. Energy Mater. Sol. Cells* **2007**, *91*, 1658–1662. [CrossRef]
206. Shaheen, I.; Ahmad, K.S.; Zequine, C.; Gupta, R.K.; Thomas, A.G.; Azad Malik, M. Sustainable synthesis of organic framework-derived ZnO NPs for fabrication of supercapacitor electrode. *Environ. Technol.* **2020**, *43*, 605–616. [CrossRef]
207. Saranya, M.; Ramachandran, R.; Wang, F. Graphene-ZnO (G-ZnO) nanocomposite for electrochemical supercapacitor applications. *Adv. Mater. Devices* **2016**, *1*, 454–460. [CrossRef]
208. Ezeigwe, E.R.; Tan, M.T.; Khiew, P.S.; Siong, C.W. One-step green synthesis of graphene/ZnO nanocomposites for electrochemical capacitors. *Ceram. Int.* **2015**, *41*, 715–724. [CrossRef]
209. Nivin, T.S.; Sindhu, S. Fabrication of novel thin film capacitor based on PVA/ZnO nanocomposites as dielectric material. *Bull. Mater. Sci.* **2020**, *43*, 1–6. [CrossRef]
210. Guo, R.; Yue, W.; An, Y.; Ren, Y.; Yan, X. Graphene-encapsulated porous carbon-ZnO composites as high-performance anode materials for Li-ion batteries. *Electrochim. Acta* **2014**, *135*, 161–167. [CrossRef]
211. Zhang, H.; Wang, Y.; Zhao, W.; Zou, M.; Chen, Y.; Yang, L.; Xu, L.; Wu, H.; Cao, A. MOF-derived ZnO NPs covered by N-doped carbon layers and hybridized on carbon nanotubes for lithium-ion battery anodes. *ACS Appl. Mater. Interfaces* **2017**, *9*, 37813–37822. [CrossRef] [PubMed]
212. Jing, M.; Li, F.; Chen, M.; Long, F.; Wu, T. Binding ZnO nanorods in reduced graphene oxide via facile electrochemical method for Na-ion battery. *Appl. Surf. Sci.* **2019**, *463*, 986–993. [CrossRef]
213. Faber, H.; Burkhardt, M.; Jedaa, A.; Kälblein, D.; Klauk, H.; Halik, M. Low-temperature solution-processed memory transistors based on ZnO NPs. *Adv. Mater.* **2009**, *21*, 3099–3104. [CrossRef]
214. Cho, S.Y.; Kang, Y.H.; Jung, J.Y.; Nam, S.Y.; Lim, J.; Yoon, S.C.; Choi, D.H.; Lee, C. Novel ZnO inks with ZnO NPs for low-temperature, solution-processed thin-film transistors. *Chem. Mater.* **2012**, *24*, 3517–3524. [CrossRef]
215. Yun, D.Y.; Kwak, J.K.; Jung, J.H.; Kim, T.W.; Son, D.I. Electrical bistabilities and carrier transport mechanisms of write-once-read-many-times memory devices fabricated utilizing ZnO NPs embedded in a polystyrene layer. *Appl. Phys. Lett.* **2009**, *95*, 267. [CrossRef]
216. Hmar, J.J.L. Flexible resistive switching bistable memory devices using ZnO NPs embedded in polyvinyl alcohol (PVA) matrix and poly (3, 4-ethylenedioxythiophene) polystyrene sulfonate (PEDOT: PSS). *RSC Adv.* **2018**, *8*, 20423–20433. [CrossRef]

217. Zhang, H.; Zhao, X.; Huang, J.; Bai, J.; Hou, Y.; Wang, C.; Wang, S.; Bai, X. Bistable non-volatile resistive memory devices based on ZnO NPs embedded in polyvinylpyrrolidone. *RSC Adv.* **2020**, *10*, 14662–14669. [CrossRef]
218. Selmi, A.; Fkiri, A.; Bouslimi, J.; Besbes, H.C. Improvement of dielectric properties of ZnO nanoparticles by Cu doping for tunable microwave devices. *J. Mater. Sci. Mater. Electron.* **2020**, *31*, 18664–18672. [CrossRef]
219. Raghunath, A.; Perumal, E. Metal oxide NPs as antimicrobial agents: A promise for the future. *Int. J. Antimicrob. Agents* **2017**, *49*, 137–152. [CrossRef]
220. Wang, S.C.; Wang, X.H.; Qiao, G.Q.; Chen, X.Y.; Wang, X.Z.; Wu, N.N.; Tian, J.; Cui, H.Z. NiO NPs-decorated ZnO hierarchical structures for isopropanol gas sensing. *Rare Met.* **2022**, *41*, 960–971. [CrossRef]
221. San Tang, K. The current and future perspectives of ZnO NPs in the treatment of diabetes mellitus. *Life sciences* **2019**, *239*, 117011. [CrossRef]
222. Patil, V.L.; Dalavi, D.S.; Dhavale, S.B.; Vanalakar, S.A.; Tarwal, N.L.; Kalekar, A.S.; Kim, J.H.; Patil, P.S. Indium doped ZnO nanorods for chemiresistive $NO_2$ gas sensors. *New J. Chem.* **2022**, *46*, 7588–7597. [CrossRef]
223. Kumar, B.; Poddar, S.; Sinha, S.K. Electrochemical cholesterol sensors based on nanostructured metal oxides: Current progress and future perspectives. *J. Iran. Chem. Soc.* **2022**, *19*, 4093–4116. [CrossRef]
224. Kwon, D.H.; Jin, E.H.; Yoo, D.H.; Roh, J.W.; Suh, D.; Commerell, W.; Huh, J.S. Analysis of the Response Characteristics of Toluene Gas Sensors with a ZnO Nanorod Structure by a Heat Treatment Process. *Sensors* **2022**, *22*, 4125. [CrossRef]
225. Sarojini, S.; Jayaram, S. An Impact of Antibacterial Efficacy of Metal Oxide NPs: A Promise for Future. *Bio-Manuf. Nanomater.* **2021**, 393–406.
226. Cao, P.; Cai, Y.; Pawar, D.; Han, S.; Xu, W.; Fang, M.; Liu, X.; Zeng, Y.; Liu, W.; Lu, Y.; et al. Au@ ZnO/rGO nanocomposite-based ultra-low detection limit highly sensitive and selective $NO_2$ gas sensor. *J. Mater. Chem. C* **2022**, *10*, 4295–4305. [CrossRef]
227. Raliya, R.; Saharan, V.; Dimkpa, C.; Biswas, P. Nanofertilizer for precision and sustainable agriculture: Current state and future perspectives. *J. Agric. Food Chem.* **2017**, *66*, 6487–6503. [CrossRef]
228. Luo, Y.; Ly, A.; Lahem, D.; Martin, J.D.; Romain, A.C.; Zhang, C.; Debliquy, M. Role of cobalt in Co-ZnO nanoflower gas sensors for the detection of low concentration of VOCs. *Sens. Actuators B Chem.* **2022**, *360*, 131674. [CrossRef]